Production of activated carbon from agricultural waste and investigation of its efficiency for textile wastewater treatment

By

Parvin Donyanavard

A thesis submitted to the Faculty of Graduate Studies of

The University of Manitoba

in partial fulfillment of the requirements of the degree of

MASTER OF SCIENCE

Department of Civil Engineering

University of Manitoba

Winnipeg Manitoba R3T 5V6

Canada

Abstract

The purpose of this study is to investigate the potential of *Moringa stenopetala* seed husks (MSSH) for making activated carbon and its applicability as an adsorbent for removing Reactive Black 5 (RB5) and Basic Blue 3 (BB3) from textile effluent. To produce activated carbon, the MSSH was first impregnated with H_3PO_4 at a ratio of 3:1 followed by pyrolysis at 400 ℃ and 500 ℃ under N_2 flow for 1 hour. BET analysis showed a higher surface area (1693 m^2/g) for the sample carbonized at the higher temperature, which was selected for the rest of the experiments. Adsorption studies were conducted at different pH, contact time, activated carbon doses, and initial dyes concentrations. Results showed that Langmuir isotherm can better describe adsorption data indicating a monolayer coverage on the adsorbent surface. The maximum monolayer adsorption capacity of prepared activated carbon was found to be 833 and 67 mg/g for BB3 and RB5, respectively, which shows the produced activated carbon has a higher affinity toward cationic dyes. Based on the kinetic studies, the adsorption of the dyes onto the prepared activated carbon well followed the pseudo-second-order kinetic model. In experiments performed with synthetic textile wastewater, 100% dye removal was achieved at pH 6 in one hour by applying 3 g/L activated carbon when the concentration of each dye was as high as100 mg/L. The results of this study revealed that MSSH can be used to produce sustainable activated carbon which is competitive to the commercial one and has high efficiency for complete dye removal from textile wastewater.

Acknowledgments

I would first like to express my sincere gratitude to my supervisor, Dr. Qiuyan Yuan, for all her continuous support, patience, and motivation throughout my study and research. I am grateful to her for keeping trust in me and giving me the opportunity to work with her and enhance my knowledge and skills. I also would like to thank my thesis committee, Dr. Jan Oleszkiewicz and Dr. Hartmut Holländer for their insightful comments and feedbacks.

I am very thankful for receiving the scholarship from the University of Manitoba Graduate Fellowship (UMGF).

I would like to show my sincere appreciation to Dr. Victor Wei for all his time and helpful guidance during my research and lab work.

I also appreciate the cooperation of the Nano-Systems Fabrication Laboratory (NSFL) director, Dr. Cyrus Shafai, and the NSFL manager Dwayne Chrusch.

Finally, I am very grateful to my dear husband, Alireza, my family and friends for all their love and kind support during this journey.

I want to dedicate my thesis to my grandmother who always encouraged me to be strong and keep going. She would be very happy if she was alive and saw my success.

Table of contents

List of Tables

List of Figures

List of Abbreviations

AC	Activated carbon
AC-400	Moringa Stenopetala Seed Husk activated carbon produced at 500°C
AC-500	Moringa Stenopetala Seed Husk activated carbon produced at 400°C
ATR	Attenuated total reflection
A.U	Absorbance Unit
BB3	Basic Blue 3
BET	Brunauer–Emmett–Teller
BJH	Barrett, Joyner, and Halenda
Ce	Liquid-phase equilibrium concentration
FTIR	Fourier transform infrared spectroscopy
GAC	Granular activated carbon
IUPAC	International Union of Pure and Applied Chemistry
k_1	Pseudo-first order constant rate
k_2	Pseudo-second order constant rate
MSSH	Moringa Stenopetala Seed Husk

PAC	Powder activated carbon
q_{max}	Maximum adsorptive capacity
q_e	Adsorptive capacity at the equilibrium
q_t	Adsorptive capacity in a given time t
RB5	Reactive Black 5
PZC	Point of Zero Charge
UV	Ultraviolet

CHAPTER 1. INTRODUCTION

Each year approximately 1.3×10^{10} metric tons of lignocellulosic biomass, including agricultural waste, are produced worldwide (Lee et al. 2014; Abdullah et al. 2017). A considerable amount of these materials are deposited in landfills, negatively affecting the environment (El-Hendawy 2005). Biomass contain organic compounds and depositing them in landfills leads to the creation of leachate and groundwater pollution. They also increase the emission of volatile organic compounds (VOCs) and greenhouse gases. As a result, diverting biomass from the disposal and recovering them would be very important from environmental protection aspects. Agricultural wastes are cellulosic, lignin, or lignocellulosic materials, and based on their sources, may contain high carbon content, multifunctional group surfaces such as carboxylic and hydroxyl, as well as bioactive agents. These properties make agricultural waste a promising option for environmental remediation, phytomedicine, and biofuel generation (Dinita et al. 2011; Inyinbor et al. 2016; Oluyori et al. 2016).

One of the high-value-added products that can be made from agricultural waste is activated carbon (AC), which refers to carbon-rich material, and as an adsorbent for pollutant removal, has numerous applications, particularly in water and wastewater treatment industries because of its unique properties including favorable pore sizes and structure as well as its high surface area (Bhatnagar et al. 2013). The surface characteristics and adsorption capacity of AC highly depend on the nature of the precursor and the activation process (Cagnon et al. 2009).

For many years, coal was believed to be the best precursor for making AC; however, coal mines are not renewable and high production cost of AC from coal has limited its application. On the other hand, bio-renewable resources, such as lignocellulosic biomass, which are abundant and

inexpensive, have a great potential for sustainable production of AC, mainly because of their high volatile matter and low ash content (Danish and Ahmad 2018; Dias et al. 2007). Having said that, three main reasons justify the production of AC from lignocellulosic biomass: 1) the unique properties of biomass, particularly in terms of surface functional groups to make a carbonaceous adsorbent, 2) the wide availability of biomass that makes the mass production of AC cost-effective, and 3) the substantial decrease in organic waste disposal due to converting biomass to value-added products which indeed benefits the environment (Chowdhury et al. 2012).

In this study, among various agricultural waste containing lignocellulosic material, the Moringa Stenopetala Seed Husks (MSSH) was selected as a precursor for producing AC, since its potential for AC production has not been studied and understood yet, while a few previous studies showed that its seed and seed husk powder have high potential as a bio-adsorbent and natural coagulant for pollutant removal from wastewater (Abiyu et al. 2018; Degefu and Dawit 2013; Gatew and Mersha 2013; Kebede et al. 2019).

Moringa is a multipurpose tree with vital nutritional, industrial, and medicinal applications that make it economically and socially significant (Council 2006; Jahn 1991). The Moringa family has different species, among which *Moringa Oleifera* and *Moringa Stenopetala* are the most common. However, despite many kinds of research that have been conducted about the potential uses of *M. Oleifera*, only a few research can be found about the potential application of *M. stenopetala* as a whole and its seed husks in particular (Abiyu et al. 2018; Degefu and Dawit 2013; Gatew and Mersha 2013; Kebede et al. 2019).

M. stenopetala, also known as "cabbage tree", is a tree endemic to East Africa, and it is extensively grown in southern Ethiopia as a food crop. Each part of this tree, such as root, stem, leaves, and seeds, is utilized for different purposes. The seed of *M. stenopetala* is considered a

significant source of oil suitable for human consumption. The seed oil can also be used in industrial applications. Based on the recent study done by Abiyu et al. (2018), *M. stenopetala* seed oil has considerable potential to be used as a raw material in producing biodiesel. During the seed processing for oil production, a significant amount of seed husk is generated, which is a lignocellulosic waste corresponding to about 25% of the seed weight (Melaku et al. 2017). A considerable portion of these seed husks is disposed of in landfills or set on fire, resulting in environmental pollution. One of the efficient utilization of this lignocellulosic biomass that can bring obvious economic and environmental benefits is its conversion to AC. Annual seed production of one *M. Stenopetala* tree can reach 6 kg, of which 25% is husk (Melaku et al. 2017). In the ideal condition, the AC production from lignocellulosic material is reported to be around 50% (Marsh and Reinoso 2006), which means annual AC production of 750 g per tree. Considering many *M. Stenopetala* trees cultivated in different regions, particularly in South Africa, the amount of waste reduction and AC production will be significant. Hence, using the seed husks as a precursor for AC production, on the one hand, decreases its waste noticeably and, on the other hand, leads to the generation of AC that can be competitive to the commercial one due to its high quality and low production cost.

After producing AC from *M. stenopetala* seed husks, among various applications of activated carbon, this research aimed to evaluate its efficiency in removing anionic and cationic dyes from textile wastewater. Many industries, including textiles, printing, rubber, cosmetics, plastics, and leather manufacturing, use different dyes to color their products, which leads to the generation of a considerable amount of colored effluent. Among these industries, textile-manufacturing companies, which apply more than 1000 tons of dyes annually, are the most dye consumers for coloring a wide variety of fibers. It was estimated that during dyeing processes in

textile industries, around 10 to 15 percent of these dyes are discharged as effluents (Reisch 1996). Synthetic dyes are among environmental pollutants with significant challenges in their removal from wastewater due to their aromatic structures, which resulted in being resistant to oxidation, chemical and biological degradation, and their stability toward the light (Banerjee and Chattopadhyaya 2017; Sepulveda and Santana 2013). Even a very low concentration of dyes in water bodies can prevent the penetration of light into the water, decreasing photosynthetic activities of aquatic life. As a result, the amount of dissolved oxygen decreases, leading to disturbance in biological processes that occur in water. Moreover, due to the toxicity of most of the dyes, their presence in water will harm organisms and aquatic life and consequently can harm humans as well (Boeniger 1980; Cox 1995). In addition, people who work in textile industries are in danger of long time exposure to the dyes, which increases the risk of bladder cancer (Mimi et al. 2002).

The dyes that are selected in this study are Reactive Black 5 (RB5) and Basic Blue 3 (BB3), which are anionic and cationic dyes, respectively. BB3 is a synthetic dye that primarily applies to textile industries for direct printing acrylic carpet, dying wool, acrylic blended fabric, and silk (Diquarternasi 2009). BB3 is among the most prevalent azo dyes in the textile sector. Reactive dyes are extensively applied to color many synthetic and natural fabrics such as silk, cotton, nylon, and wool because of their high level of interaction with the fabric surfaces (Mottaleb and Littlejohn 2001). However, the most common application of reactive dyes is for coloring cotton, which constitutes almost half of the world's fiber consumption (Vandevivere et al. 1998). The fixation rate of reactive dyes is about 60-70% (Carr 1995). As a result, 30-40% of hydrolyzed dye remained unfixed in the bath after the reactive dyeing process, making the effluent highly colored. It is reported that the human eye could detect even a small concentration of reactive dyes, i.e., 0.005

mg/L, in water. Therefore, concentrations more than this amount would not aesthetically be permitted (Pierce 1994).

The conventional treatment methods, such as coagulation, flocculation, and biological methods, have been shown to be insufficient for complete dye removal. In contrast, adsorption methods have been reported as a promising option to decolorize textile wastewater provided that low-cost AC such as those produced from waste is applied to make the adsorption method cost-effective (Santhy and Selvapathy 2006).

The objectives of this research were firstly production of activated carbon from *M.Stenopetala* seed husk and then among various applications of AC, this research focused on its efficiency to remove dyes, in particular Reactive Black 5 (as an anionic dye) and Basic Blue 3 (as a cationic dye) from synthetic textile wastewater.

CHAPTER 2. LITERATURE REVIEW

2.1. Textile industry

Textile industries produce fibers under dry and wet techniques. The latter consists of sizing, de-sizing, sourcing, bleaching, mercerizing, dyeing, printing, and finishing processes (Babu and Parande 2007; Wang et al. 2011). Among these processes, the dyeing step is of great importance in textile production. During this process, different dyes are used to color fibers, and a number of chemicals may be applied to enhance the fixation between dyes and fibers, such as metals, salts, surfactants, organic processing aids, sulfide, and formaldehyde (Yaseen and Scholz 2019). The dying process also consumes a significant amount of potable water. It is estimated that dying processes of 12 to 20 tons of textiles per day lead to the generation of 1000 to 3000 m^3 wastewater (Al-Kdasi et al. 2004; Pagga and Brown 1986). There is always a portion of dyes that are not fixed onto the fibers during dyeing processes which makes the remaining water very colored. Colored effluent not only causes receiving water bodies to be aesthetically undesirable but also negatively affects the environment since most of these dyes are toxic and non-biodegradable (US EPA 1996). Therefore, dyes must be removed before discharging the colored effluent to the water bodies.

2.2. Dyes classification

Dyes are coloring agents with chemical compounds that bind to fabrics or surface shells to give them color. Nowadays, most of the dyes are synthetically made, while in the past, plants, animals, and minerals were used to produce natural colorants. Approximately 10,000 dyes are commercially available that can be used in textiles, paper, rubber, plastics, leather, cosmetics, pharmaceutical, and food industries. Each year almost 7×10^5 tons of various dyes are produced worldwide (Chowdhury et al. 2011; Gupta et al. 2008). As a result, it is of great importance to

classify dyes due to the existence of several kinds and a large number of colorants. Dyes are mainly categorized based on their chemical structure or according to their mode of application. The former classification includes azo, anthraquinone, indigo, phthalocyanine, sulfur, nitro, and nitroso dyes. Azo dyes constitute almost 60–70% of all dyes utilized by the textile industries (Dutta et al. 2016; He et al. 2012). In terms of application methods, dyes can be categorized as reactive, disperse, acid, basic, direct, and vat dyes (Gürses et al. 2016). Dyes can also be cationic or anionic according to their charge. While the positive charge is attributed to protonated amine or groups containing sulfur, sulphonate causes the negative charge of anionic dyes (Khatri et al. 2015).

The types of dyes and chemicals used in the textile industry depend on the fabrics to be colored. Fabrics can be produced from cellulosic materials such as cotton, rayon, and linen, or they can be obtained from animals as protein fibers such as wool, silk, and mohair. There are also other types of fabrics that are artificially produced, named synthetic fibers, including nylon, polyester, and acrylic (Yaseen and Scholz 2019). Cellulose fibers can be colored with dyes such as Reactive, direct, naphthol, and indigo. Reactive dyes are the most common dye applied, particularly for dyeing cotton (Keane and te Velde 2008; Lorimer et al. 2001; Robert et al. 2008). Protein fibers are mostly dyed with acid dyes. These dyes chemically react with the fibers, and the dye molecule that formed on the fiber is insoluble (Valko 1957). Synthetic fibers, including polyester, nylon, or acetates, are mostly dyed with dispersed dyes (UNSD 2013). However, the coloring of Nylon fibers and acrylic fibers would be more effective using direct dyes and basic dyes, respectively (Burch 2013).

2.3. Textile wastewater treatment methods

Various treatment methods have been used to remove dyes from textile wastewater, which can be categorized as physical, chemical, and biological methods. Majority of dyes have complex aromatic molecular structures that render them stable to photo-degradation, bio-degradation, and oxidizing agents (Ramakrishna and Viraraghavan 1997). Therefore, physical or chemical methods have been a center of attention in various research for dye removal from textile wastewater. In spite of the efficiency of chemical methods in removing dyes, a huge number of by-products will be generated mainly due to the utilization of different chemicals, which leads to the production of high sludge volume after treatment. In addition, these treatment methods are very energy-intensive and need specialized equipment as well (Robinson et al. 2001). By contrast, physical treatment methods including adsorption, ion exchange, and membrane filtration, do not have the problem of by-product generation and they have been shown to be more effective for dye removal compared to the chemical and biological methods (Vandevivere et al. 1998). Among physical treatment methods, many researchers have investigated removing anionic and cationic dyes by adsorption on different natural adsorbents, particularly activated carbon due to its simplicity of design, easy operation, and low initial cost (Crini 2006; Faria et al. 2004; Janoš et al. 2003).

2.4. Adsorption

Adsorption is a process in which atoms, molecules, or ions accumulate at the interface of two phases like solid and liquid or solid and gas (Tareq et al. 2019). Thus, in the liquid phase, i.e., water and wastewater, undesired substances can be adsorbed on a solid phase and eliminated from the solution. The constituent that is adsorbed on the solid is known as the adsorbate, and the solid is named adsorbent.

2.4.1. Adsorption Isotherms

If the adsorbate and adsorbent are contacted long enough, an equilibrium distribution of adsorbate between the solid and liquid phases will be established. Then the concentration of the adsorbate in the liquid phase can be determined spectrophotometrically and compared to the initial adsorbate concentration. Many mathematical relationships can describe the equilibrium relationship. These relationships are referred to as adsorption isotherms since they are only applicable when the temperature is constant during adsorption tests. Among isotherm equations, Langmuir and Freundlich have been widely applied for adsorption modeling (Sharma and Upadhyay 2011).

Langmuir isotherm model can be applied to describe adsorption data. The assumptions of this model are: 1) Points of valency exist on the adsorbent surface; 2) Only one molecule can be held by each site (monolayer coverage only); 3) The affinity of all adsorption sites is equal for the adsorbate molecules; 4) Adsorbate molecules on near sites do not have any interaction with each other. On the other hand, when the surface of the adsorbent is heterogeneous, adsorption data can be analyzed by Freundlich isotherm model (Freundlich, 1907).

2.4.2. Kinetics of adsorption

Adsorption process is progressed through four steps: 1) The movement of adsorbate from the liquid bulk toward the thin film exists around the adsorbent particle; 2) The transportation of adsorbate from the adsorbent film to its external surface (film or external diffusion); 3) Adsorbate species transfer to the adsorbent interior particles (intraparticle diffusion or internal diffusion) through a pore or surface diffusion; 4) Energetic interaction between the adsorbate molecules and

the final adsorption sites. Total adsorption rate is controlled by the film and/or intraparticle diffusion (the slower process) since the first and last steps are done very fast (Worch 2012).

2.4.2.1. Kinetic Models

Kinetic adsorption studies are necessary for identifying the optimum and efficient operating conditions for the industrial scale. Kinetic models indicate the rate of adsorbate uptake, which controls the solute dwell time at the solid-solution interface. Among several kinetic models, the pseudo first-order, the pseudo second order, Elovich and intraparticle diffusion has been widely applied by researchers. The compliance between values from the kinetic model prediction and experiments is illustrated by the correlation coefficients (R^2). The higher R^2 values (close or equal to 1) indicate the better description of solute adsorption kinetics by the model (Malik 2004).

2.4.3. Chemisorption versus physisorption

Accumulation of dissolved species on the solid surface can happen through a chemical reaction (chemisorption) or physical attraction (physisorption) to the surface. Physisorption, the most common mechanism in adsorbates removal from the aqueous phase, is a rapid process that occurs due to the week van der Waals forces without any exchange of electrons. This process is reversible, which means the adsorbate desorbs from the solid surface if its concentration in the solution becomes lower than that on the solid surface. The physical adsorption process is exothermic with adsorption heat generally ranging from 4 to 40 kJ/mol (Crittenden et al. 2012).

In chemisorption, a chemical reaction with the surface occurs because electrons are transferred between the adsorbate and adsorbent. The heat of adsorption for chemisorption generally exceeds 200 kJ/mol (Crittenden et al. 2012).

2.4.4. Adsorbent types

Adsorbents applied for water and wastewater treatment can be classified as natural and synthetic adsorbents. While the former has a natural origin like minerals, natural zeolites, oxides, or biopolymers, the latter is prepared from different kinds of wastes, including household wastes, agricultural and industrial wastes, sewage sludge, and polymeric adsorbents. Many adsorbents' characteristics, such as their pore structure and porosity and their surfaces' nature and functional groups, are specific to each adsorbent. Among different adsorbents, activated carbon is the most common adsorbent used in water and wastewater treatment (Rashed 2013).

2.5. Activated Carbon production

A variety of carbon-based materials can be used to produce activated carbon. The internal pore structure, as well as the surface area and the surface chemistry of the produced AC, are highly dependent on the type of precursor and the activation process (González-García 2018). Conversion of raw material to the AC can be done through two main routes: physical activation and chemical activation.

In physical activation (also called thermal activation), first, the precursor carbonized under an inert atmosphere (pyrolysis) at temperatures ranging from 400 ℃ and 850 ℃ to remove organic compounds and produce a solid residue with high carbon content. In the next step, which is activation, the carbonized material undergoes slow oxidation with mild oxidizing agents such as steam and carbon dioxide at temperatures usually between 800 ℃ and 900 ℃. This process leads to the creation of new pores and enlarging the existing pores. Compared to steam, carbon dioxide has lower reactivity that allows the better control of oxidation rates which develops uniform porosity (González-García 2018).

In chemical activation, dehydrating agents such as H_3PO_4, H_2SO_4, HNO_3, $ZnCl_2$, and KOH are used to impregnate the raw precursor and prevent the tar and other unwanted products from forming in the process of carbonization. Application of chemical agent also develops the precursor porosity by dehydrating and degrading its structure. After drying the precursor-agent mixture under 110 ℃, the char undergoes pyrolysis at temperature ranges from 400 ℃ to 1000 ℃ under an inert atmosphere such as nitrogen to generate and develop the internal porosity in the precursor better. The final product should be washed extensively to remove chemical agents (González-García 2018). Although washing and removing chemicals at this stage might be considered a drawback for this method (with respect to the environment), chemical activation requires a lower temperature than physical activation, and the yield is also higher (Contescu et al. 2018).

According to the particle sizes, there are two other categories of AC: powdered activated carbon (PAC) and granular activated carbon (GAC). PAC has smaller particle sizes (20 - 50 μm), but a higher surface area (1400 to 1800 m^2/g) compared to GAC which has particle sizes of 0.5 to 3 mm and surface area of 950 to 1075 m^2/g (Crittenden et al. 2012).

2.6. Application of activated carbon

Activated carbon is an efficient adsorbent that can remove a variety of organics and inorganics from gaseous and liquid media, particularly water and wastewater, due to its noticeable surface area, well-built pore structure, effective pore sizes, and a broad range of surface functional groups (Yahya et al. 2015). The most common applications of AC from 1985 to 2016 were reported for removing heavy metals (59.95%), dyes (8.47%), organics (7.41%), catalyst (6.77%), and CO_2 capture (5.82%) (González-García 2018).

2.7. Textile wastewater treatment by waste-derived activated carbon

Due to the paramount importance of solid waste management and converting waste to valuable products such as activated carbon, many studies have been conducted on AC production from biomass and agricultural waste and its applicability for different purposes such as pollutant removal from wastewater. However, no work has been reported previously on the potential of *M. stenopetala* seed husks for AC production. Some of the achievements in producing waste derived AC to remove dyes from colored wastewater are as follows:

2.7.1. Removal of cationic dyes by waste-derived activated carbon

Nor Salmi et al. (2017) studied the optimal condition to produce AC from *Moringa Olifera* seed pod. Based on their result, the precursor should be chemically activated with $ZnCl_2$ and then carbonized at 800ºC in a furnace with nitrogen flow. This process resulted in producing AC with a BET surface area of 853.68 m^2/g, with which a 90.7 % of methylene blue removal was observed (Abdullah et al. 2017).

Sunflower oil cake was used by Karagöz et al. (2008) for AC production. The precursor was first activated by sulfuric acid with different impregnation ratios (0, 0.85, 1.9) followed by carbonization at 600 ℃. Then adsorption experiments were performed to determine the effectiveness of produced AC in removing methylene blue (MB) from aqueous solutions. Their results showed that carbons impregnated with the ratio of 0.85 showed better performance. Furthermore, experimental data fitted well with the Langmuir isotherm and pseudo-second-order kinetic models. They obtained a maximum adsorption capacity of 16.43 mg MB per gram of activated carbons at pH of 6 (Karagöz et al. 2008).

García et al. (2018) conducted research to produce AC from palm kernel shells (PKS), which were then tested for methylene blue (MB) removal from colorant water. The palm kernel shell was activated by $ZnCl_2$ with mass ratios of 1:1 and 1:2, followed by carbonization at 500 ℃ and 550 ℃ for 1 hour. Their result showed that the maximum adsorption capacity of 225.3 mg/g was achieved due to the high specific surface area (2058 m^2/g) when the precursor was prepared with 1:1 (PKS: $ZnCl_2$) and carbonized at 550 °C. They also reported over 90 % removal of methylene blue when the initial dye concentration was 200 mg/L without pH adjustment (García et al. 2018).

García et al. (2018) conducted research to produce AC from palm kernel shells (PKS), which were then tested for methylene blue (MB) removal from colorant water. The palm kernel shell was activated by $ZnCl_2$ with mass ratios of 1:1 and 1:2, followed by carbonization at 500 ℃ and 550 ℃ for 1 hour. Their result showed that the maximum adsorption capacity of 225.3 mg/g was achieved due to the high specific surface area (2058 m^2/g) when the precursor was prepared with 1:1 (PKS: $ZnCl_2$) and carbonized at 550 °C. They also reported over 90 % removal of methylene blue when the initial dye concentration was 200 mg/L without pH adjustment (García et al. 2018).

Hameed and Daud (2008) studied Basic Blue 3 from an aqueous solution by AC produced from rubber (*Hevea brasiliensis*) seed coat. Initially, carbonization of the precursor was conducted at 700 ℃ under nitrogen flow for 2 hours. Then it was washed with potassium hydroxide pallets (ratio 1:1) followed by activating at 850 ℃ under carbon dioxide flow for 2 hours. The produced AC reported to have BET surface area and the total pore volume of 1225 m^2/g and 0.85 cm^3/g, respectively. Adsorption isotherm studies indicated that the Freundlich model could describe the experimental data very well resulted in a monolayer adsorption capacity of 227.27 mg/g at 30℃.

Pseudo-second order was also found to be the best kinetic model to describe the adsorption kinetics (Hameed and Daud 2008).

Ahmed et al. (2018) studied the potential of AC produced from rice husk for dye removal from tannery wastewater. The AC was applied as an adsorbent in laboratory batch tests with methylene blue and tannery wastewater. The results showed the color removal of 94.13% for methylene blue and 77% for tannery wastewater. Although the experimental adsorption process was represented reasonably well by both Langmuir and Freundlich isotherms, the Langmuir model fitted better, indicating the possibility of monolayer adsorption (Ahmed et al. 2018).

2.7.2. Removal of anionic dyes by waste-derived activated carbon

Malik (2004) developed AC from Mahogany sawdust by carbonization and then activation of the precursor at 500 ℃ and 800 ℃ for 1 hour, respectively. He investigated the removal of direct dyes (Direct Green B and Direct Blue 2B) from textile wastewater by the AC. The data from experiments were more in line with the Langmuir isotherm and pseudo-second-order model. The equilibrium adsorptive capacity determined by these models reported to be 300 – 500 mg per gram of produced AC. He reported a pH of 3 and below as the best pH for direct dyes adsorption on sawdust carbon (Malik 2004).

Orange peel was impregnated by H_2SO_4 and used to produce AC by Khaled et al. (2009). They tested the prepared AC for Direct N Blue-106 removal from synthetic textile wastewater. The adsorption data showed good consistency with both Langmuir and Freundlich models (R^2 > 97). Based on their result, when the DNB-106 concentration is 150 mg/L, carbon dosage is 2 g/L, and the pH is 2, the maximum adsorptive capacity would be 107.53 mg/g. In this experiment condition, they reported more than 75% DNB-106 removal in 3 hours. Based on their result, the

best model representing the adsorption kinetics was the pseudo-second-order model (Khaled et al. 2009).

In research carried out by Namasivayam and Kavitha (2002), AC production from coir pith was studied for Congo Red removal from aqueous solution. Initially, to carbonize the precursor, it was placed in a muffle furnace at 700℃ for 1 hour and then sieved to 250 –500 micron. Their result showed that adsorption data could be described by both Langmuir and Freundlich isotherms very well. Kinetic studies revealed that adsorption data is consistent with the pseudo-second-order model. They reported the maximum adsorption capacity of 6.72 mg/g in acidic pH (Namasivayam and Kavitha 2002).

Santhy and Selvapathy (2006) evaluated the removal of three reactive dyes, including Reactive Orange 12, Reactive Red 2, and Reactive Blue 4, from textile wastewater by AC produced from coir pith. The coir pith was first impregnated by sulfuric acid and then activated at 900 ℃ in the presence of carbon dioxide for 30 min. Their result showed a higher affinity of the prepared AC for Reactive Orange, which decreased for Reactive Red and Reactive Blue 4, respectively. Acidic pH was reported as a favorable condition for maximum removal of all the dyes. Freundlich and pseudo-first-order models were found to be the best isotherm and kinetic models, respectively, for adsorption of dyes (Santhy and Selvapathy 2006).

Pelaez-Cid et al. (2016) prepared mesoporous AC from three vegetable residues: prickly pear peels (CarTunaQ), broccoli stems (CarBrocQ), and white sapote seeds (CarZapQ) to remove dyes from textile wastewater. By conducting adsorption studies in batch systems and adjusting the experimental data with Langmuir and Freundlich isotherms, CarBrocQ was found the best carbon derived with similar efficiency to the commercial one for textile dyes removal. Their result showed

high total pore volume (1.06 - 2.16 cm^3/g) with average pore size diameters between 4.1 and 8.4 nm and a large specific surface area (1025-1177 m^2/g) for produced AC (Peláez-Cid et al. 2016).

CHAPTER 3: MATERIALS AND METHODS

3.1. Preparation of activated carbon

Moringa Stenopetala Seed Husk (MSSH) was bought from BioTEI Inc., and the activated carbon was produced from MSSH based on the methodologies applied in previous studies for other agricultural waste (Ferraz and Yuan 2020; Hameed and Daud 2008; Karagöz et al. 2008; Reffas et al. 2010). Initially, the precursor (MSSH) was washed with deionized water to remove contaminants, then dried at 105 °C for 24 h, and after being cooled down to room temperature, it was sieved at 0.850-1.4 mm. This particle size was chosen based on the study of Lori et al. (2010). It was also found that if the precursor sieved to very small particles, i.e., less than 0.850 mm, it causes a significant loss during pyrolysis at high temperatures. On the other hand, particle sizes bigger than 1.4 mm were not impregnated very well, making them unsuitable for the next step, which is pyrolysis at high temperatures. As a result, optimum particle sizes were found to be in the range of 0.850-1.4 mm.

Afterward, a chemical activation method was applied to produce AC, which is carried out by impregnating the precursor, i.e., MSSH, with a chemical agent. This activation method has been preferred over the physical activation method because not only will the yield be higher, but also the surface area of the produced AC will be larger, and the porous structure will be developed better (Abdullah et al. 2017). In this study, among different activation agents available for this purpose, such as hydrochloric acid (HCl), phosphoric acid (H_3PO_4), sulphuric acid (H_2SO_4), nitric acid (HNO_3), zinc-chloride ($ZnCl_2$), and sodium hydroxide ($NaOH$), phosphoric acid (H_3PO_4) was selected as an activating agent due to a number of reasons. First of all, it is a Brönsted acid that promotes bond cleavage more effectively than other activating agents. In addition, Phosphoric acid has a non-polluting character compared to some other agents such as zinc chloride. It can also be

removed simply through water washing and recycled for further application. Another merit of using phosphoric acid as an activating agent is that, depending on the activation temperature, microporous and mesoporous carbon is better developed with a high specific surface area (Jagtoyen and Derbyshire 1998; Reffas et al. 2010; Nakagawa et al. 2007). The efficiency of activation with phosphoric acid in the production of activated carbons from various lignocellulosic precursors such as corncobs, peanut hulls, and the coffee ground has also been discussed in previous studies (El-Hendawy et al. 2001; Girgis et al. 2002; Reffas et al. 2010; Ferraz and Yuan 2020).

To impregnate MSSH, 5 grams of it were soaked in specific volumes of phosphoric acid 85% to reach the impregnation ratio of 3:1 (mass of acid: mass of precursor). This impregnation ratio was found to be optimum, as with the lower impregnation ratio, the MSSH could not be impregnated very well. A higher amount of acid also is not suggested as it prevents the development of microporosity and promotes the formation of mesopores and macropores (Zuo et al. 2010). It is also considered to have a negative effect on the yield (Mui et al. 2010) and leads to the production of activated carbons with lower adsorption capacity (Ferraz and Yuan 2020; García et al. 2018; Karagöz et al. 2008).

After mixing phosphoric acid and MSSH with the impregnation ratio of 3:1, it was shaken very well and then sonicated for one hour. Then the samples were dried at 105 °C for 24 hours, and after cooling down to room temperature, weighed and kept in a desiccator for the next step, which is pyrolysis. In this study, pyrolysis was carried out using a Lindberg Blue M box furnace. Samples were placed inside the furnace for one hour under a steady nitrogen flow at two different temperatures, 400 °C, and 500 °C. For lignocellulosic materials activating with phosphoric acid, a temperature range between 400 °C and 500 °C were found to be optimum to produce high-quality

AC (Girgis et al. 2007). Although higher temperatures might enhance the quality of produced char by increasing ash and fixed carbon content and decreasing the amount of volatile matter, however, it noticeably decreases the yield of char (Ioannidou and Zabaniotou 2007).

When 1-hour pyrolysis finished, the samples were kept in the furnace and allowed to cool down to room temperature under the N_2 flow and then weighed. Finally, the samples were washed several times with distilled water to remove any remaining acids. Then, samples were mixed with 0.1 M hydrochloric acid (HCl) for one hour to remove any residual ash and metal oxides. Afterward, 0.1 M sodium bicarbonate ($NaHCO_3$) was added to the samples to remove any remaining acids from the previous steps. Then samples were rewashed with distilled water and rinsed until the pH of the remaining solution reached neutral (6-7). Finally, the samples were dried at 105 °C for 24 h, and after getting the room temperature, weighed, grind to a fine powder (< 250 µm) and kept in an appropriate storage bottle. In the end, the percentage of activated carbons yield and burn-off was determined based on the following equations:

$$\text{Yield (\%)} = [m_{AC}/m_{MSSH}] \times 100 \quad (1)$$

$$\text{Burn off (\%)} = [m_{loss}/m_{MSSH}] \times 100 \quad (2)$$

Where m_{AC} is the final mass of AC (mg), m_{MSSH} is the initial mass of MSSH (mg) , m_{loss} is the difference between the initial mass of MSSH and the final mass of AC (mg) (Ching et al. 2011; Tehrani et al. 2015).

3.2. Adsorbent characterization

The functional groups that exist on the surface of MSSH and MSSH activated carbon was characterized by Fourier transform infrared spectroscopy (FTIR) with the application of a Bruker Tensor 27 FTIR spectrometer equipped with a KBr beam splitter and a DLATGS detector.

2.5 mg of sample and 152.5 mg of crystalline KBr were ground to uniform grain size and pelletized at 10T of pressure. Mixtures with 5 mg of sample and 150 mg of KBr were analyzed but showed significant saturation in the OH-stretching region and thus 2.5 mg of sample was used instead. Spectra over the range 4000–400 cm^{-1} were collected by averaging 100 scans at an operating resolution of 4 cm^{-1}. Base-line corrections were done using the OPUS software and absorption due to atmospheric CO_2 transitions were removed using the OPUS software (García et al. 2018).

To determine the textural properties of the produced activated carbons, nitrogen adsorption-desorption isotherms at -196 ℃ were conducted using a Mike ASAP2460 BET analyzer. Based on the isotherms analysis, the specific surface area (S_{BET}) was determined by Brunauer- Emmett-Teller (BET) equations, the total pore volume was calculated by the amount of nitrogen adsorbed at P/P0 = 0.99 and the micropore volume and external surface area obtained from V-t-method (García et al. 2018). In addition, to determine the pore size distribution, Barrett, Joyner, and Halenda (BJH) method was applied.

3.3. Determination of pH_{pzc}

One of the solution parameters that profoundly influences the adsorption of adsorbates by activated carbon is pH due to its effect on the surface properties of the adsorbent and the ionization and dissociation of the adsorbate molecules (Malik 2004). The type of active sites of adsorbent and its adsorption ability is determined by an important parameter that is the point of zero charge (PZC) (Malik 2004). The pH in which the net charge of the adsorbent surface is neutral is considered as pH_{PZC}. This value is used to understand the surface electrokinetic properties. Generally, the charge of the adsorbent surface would be positive when $pH < pH_{PZC}$ and negative when $pH > pH_{PZC}$ (Liu et al. 2013). pH_{PZC} is to be determined experimentally for each specific

adsorbent. In this study, pH_{pzc} was determined based on the previous studies by the so-called pH drift method (Faria et al. 2004; Rivera-Utrilla et al. 2001). Five Erlenmeyer flasks were filled with 50 ml of Sodium Chloride solution (0.01 M), and the solutions' pH were adjusted to 2, 4, 6, 8 and 10 by adding HCl 0.1M or NaOH 0.1M. Then, in each flask, 0.15 g of prepared activated was added and agitated for 24 hours at room temperature. Afterward, the final pH of each solution was measured, and a curve of pH final versus pH initial was plotted. The point at which this curve crosses the line of $pH_{final} = pH_{initial}$ is the pH_{pzc} (Faria et al. 2004).

3.4. Preparation of RB5 and BB3 dye solution

Two dyes from different classes, including Reactive Black 5 (RB5) and Basic blue 3 (BB3), were purchased from Sigma–Aldrich and used to evaluate the adsorption capacity of the prepared activated carbon. The characteristics of these dyes are shown in Table 1. A 1 g/L stock solution of each dye was prepared by mixing 1 gram of dyes with 1 liter of distilled water. The solution is kept in a dark place to prevent the decolorization that might occur by direct sunlight. RB5 and BB3 dye solutions with different concentrations were made from the stock solutions, and their absorbance was measured using Altrospec 2100 pro UV-Visible spectrophotometer at their maximum absorption wavelength (λ_{max}) of 597 nm and 654 nm, respectively. Then the standard calibration curves were generated, which represent the relation between absorbance data of RB5 and BB3 solutions and their corresponding concentrations (Fig. 1).

Table 1. Properties and characteristics of RB5 and BB3.

	Reactive Black 5 (RB5)	Basic Blue 3 (BB3)
Molecular formula	$C_{26}H_{21}N_5Na_4O_{19}S_6$	$C_{20}H_{26}ClN_3O$
Molecular weight (g/mol)	991.82	359.89
λ_{max} (nm)	597	654
Chemical structure	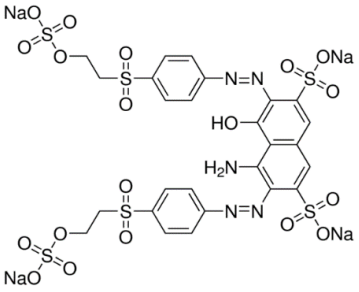	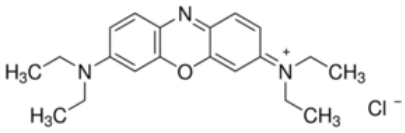

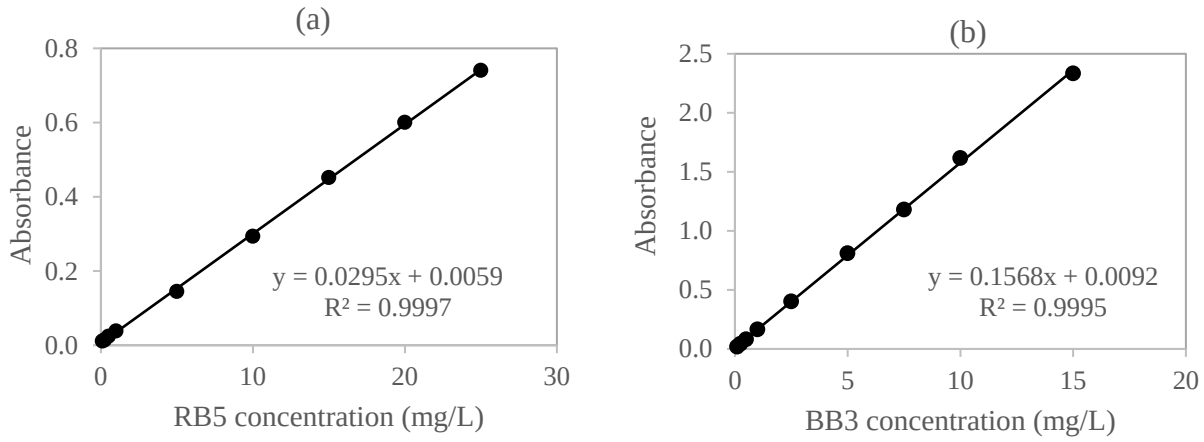

Fig. 1. Calibration curves for (a) RB5 (at λ_{max} = 597 nm) and (b) BB3 (at λ_{max} =654 nm).

3.5. Preparation of synthetic textile wastewater

Textile wastewater was synthetically made based on the previous studies (Indu et al. 2017; Sahinkaya 2013). The composition of the synthetic textile wastewater is provided in Table 2.

Table 2. Composition of synthetic textile wastewater

Chemical	Concentration (mg/L)
Reactive Black 5	100
Basic Blue 3	100
NaCl	1500
Na_2CO_3	500
$NaHCO_3$	500
NaOH	500
H_2SO_4	800
Starch	500

In the synthetic textile wastewater containing a mixture of two days, named A and B, with wavelengths of λ_1 and λ_2, and optical densities of d_1 and d_2, respectively, the remain dyes concentrations (C_A and C_B) are calculated by the following equations (Mahmood et al. 2011):

$$C_A = (K_{B2}\, d_1 - K_{B1}\, d_2) / (K_{A1}\, K_{B2} - K_{A2}\, K_{B1}) \quad (3)$$

$$C_B = (K_{A1}\, d_2 - K_{A2}\, d_1) / (K_{A1}\, K_{B2} - K_{A2} K_{B1}) \quad (4)$$

Where k_{A1}, k_{B1}, $k_{A2,}$ and k_{B2} are the calibration constants for dyes A and B at the wavelengths λ_1 and λ_2, respectively.

For Reactive Black 5 and Basic Blue 3, these calibration constants can be found from Fig. 1 and Fig. 2.

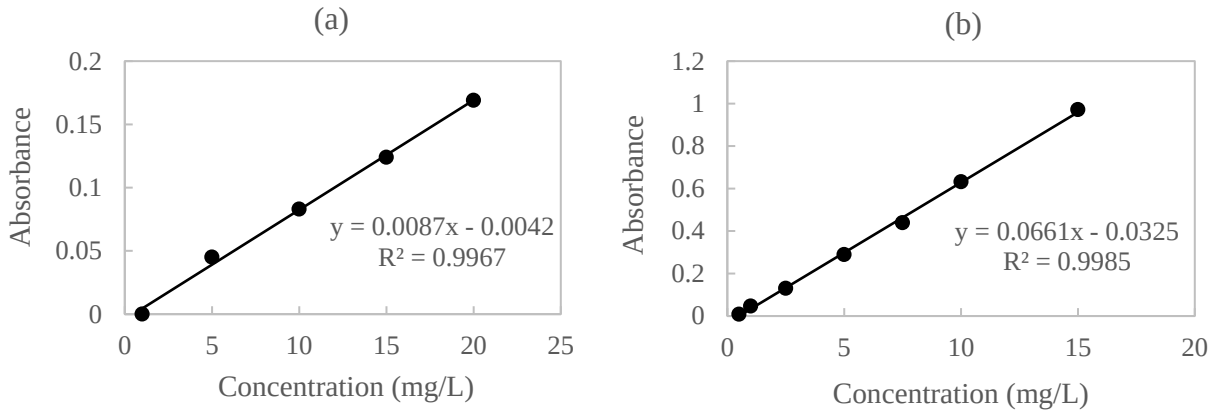

Fig. 2. Calibration curves for (a) RB5 (at λ_{max} = 654 nm) and (b) BB3 (at λ_{max} = 597 nm).

3.6. Batch adsorption studies

Batch adsorption studies were carried out to investigate the effect of different parameters, including pH, contact time, AC dosage, and initial dye concentrations, on the adsorption process. All the experiments were duplicated, and the average values are reported as less than ±5% of deviation was observed in the data. Experiments with negative controls (without AC) were also carried out to ensure that this is the AC that adsorbs dye molecules, not the container.

To determine the effect of solution pH on adsorption of dyes on AC, batch tests were performed by preparing 50 ml of RB5 and BB3 solutions with initial concentrations of 50 mg/L separately in five conical flasks (250 ml). The pH of flasks was carefully adjusted to 2, 4, 6, 8, and 10 using a small amount of 1M HCl or NaOH solution. Then equal doses of 2 g/L and 0.1 g/L of AC were added to RB5 and BB3 solutions, respectively. The solutions were kept in an orbital shaker (30±1 ℃, 200 rpm) for 2 hours. The same procedure was followed to see the results after 24 hours of contact time as well. After completion of each test, the samples were centrifuged at

12000 rpm for 5 minutes and filtered with a 0.45 µm filter. Then the absorbance of the solutions was measured using the spectrophotometer. Based on the absorbance data and dyes' calibration curves, the final concentration of each dye solution was determined.

The effectiveness of the adsorption process can be determined by an important factor, which is the adsorptive capacity (q_e). It is defined as the amount of adsorbate that can be absorbed in equilibrium per unit mass of the adsorbent. Adsorptive capacity was calculated by conducting adsorption batch tests and using the following equation:

$$q_e = \frac{(C_0 - C_e)V}{w} \quad (5)$$

where Co and Ce are the initial and equilibrium concentrations of the dye (mg/L), respectively. V is the solution volume (L), and W is the mass of adsorbent (g).

When the optimum pH was determined from the batch tests, it was used for the subsequent adsorption experiments, which were conducted at various time intervals in order to determine the adsorption equilibrium time and the maximum removal of RB5 and BB5. The experiment was also conducted to investigate the effect of different AC doses as well as different initial dye concentrations (50 – 200 mg/L).

3.7. Adsorption Isotherms

In this work, adsorption isotherms at 30 °C were studied by mixing 50 ml of RB5 and BB3 dye solutions of different concentrations (50 - 150 mg/L) with a fixed dose of AC. Samples were mixed for 24 hours, followed by centrifuging at 12000 rpm for 5 minutes. Afterward, the remaining dye concentration in the solution was measured with a spectrophotometer, and the adsorption equilibrium data were analyzed using Langmuir and Freundlich isotherm models.

3.7.1. Langmuir isotherm

Langmuir isotherm equation is shown as (Langmuir 1916; Benefield et al. 1982):

$$q_e = \frac{q_m K_L C_e}{1 + K_L C_e} \quad (6)$$

Where q_e is the amount of adsorbate adsorbed onto AC at equilibrium (mg/g), K_L is the Langmuir constant (L/mg), q_m is the maximum adsorption capacity (complete monolayer coverage on the surface) (mg/g) and Ce is the equilibrium concentration of the adsorbate (mg/L).

The following equation is the linearized form of equation (6):

$$\frac{C_e}{q_e} = \frac{1}{Q_m K_L} + \frac{C_e}{Q_m} \quad (7)$$

From the slope and intercept of the linear plot of Ce/q_e versus Ce, Langmuir constants, i.e., K_L and q_m can be determined, respectively.

Essential characteristics of the Langmuir isotherms and the nature of the adsorption process can be expressed by a dimensionless separation factor (R_L) (Weber and Chakravorti 1974):

$$R_L = \frac{1}{(1 + K_L C_0)} \quad (8)$$

where K_L is the Langmuir isotherm constant (L/mg), and Co is the initial dye concentration (mg/L). The value of R_L implies whether the nature of the adsorption process is irreversible ($R_L = 0$), favourable ($0 < R_L < 1$), linear ($R_L = 1$) or unfavourable ($R_L > 1$) (Weber and Chakravorti 1974).

3.7.2. Freundlich Isotherm

Freundlich isotherm equation (Freundlich, 1907), is given by the following equation:

$$q_e = K_F C_e^{\frac{1}{n}} \quad (9)$$

Where q_e is the amount of adsorbate adsorbed onto AC at equilibrium (mg/g), C_e is the equilibrium concentration of the adsorbate (mg/L), K_F and 1/n are equation constants indicating adsorption capacity and adsorption intensity, respectively. Generally, increasing K_F implies an increase in adsorption capacity. Stronger adsorption intensity is correlated with higher values of n. Generally, n values more than 1 (or generally between 1 and 10) indicate favorable adsorption conditions (Ahmad and Alrozi 2011).

Taking logarithms from Eq. (9) converts it to linearized form as follow:

$$\ln q_e = \ln K_F + \frac{1}{n} \ln C_e \quad (10)$$

Freundlich constants n and K_F can be calculated from the slope and intercept of the linear plot of ln q_e versus ln C_e (Fig. 2), respectively.

3.8. Kinetic Models

In this work, adsorption kinetic studies were conducted using pseudo-first order and pseudo-second order kinetic models. The experiments were performed at 30 °C using RB5 and BB3 dye solutions with an initial concentration of 50, 100, 150, and 200 mg/L and at different time intervals.

3.8.1. The pseudo-first order model

The linearized integral form of the pseudo-first-order model (Muhammad et al. 1998) is expressed as:

$$\log (q_e - q_t) = \log(q_e) - \frac{K_1}{2.303} t \quad (11)$$

Where; q_t and q_e are the adsorption capacities at time t and at equilibrium, respectively (mg/g), K_1 is the adsorption rate constant of the pseudo-first-order model (min^{-1}) and t is the contact time (min). K_1 and predicted q_e can be derived from the slope and intercept of the linear plot of log $(q_e - q_t)$ versus t, respectively.

3.8.2. The pseudo-second order model

The pseudo-second order adsorption kinetic rate equation is expressed as (Lagergren 1898):

$$\frac{dq_t}{dt} = k_2 (q_e - q_t)^2 \quad (12)$$

Where; K_2 (g min mg $^{-1}$) is the second-order rate constant of adsorption. Integrating Eq. (12) for the boundary conditions $q_t = 0 - q_t$ at t = 0 − t, is simplified and linearized to get:

$$\frac{t}{q_t} = \frac{1}{k_2 q_e^2} + \frac{1}{q_e} t \quad (13)$$

By considering the initial adsorption rate as h (mg/g/min), we have:

$$h = k_2 q_e^2 \quad (14)$$

Then Eqs. (13) and (14) would be as follows:

$$\frac{t}{q_t} = \frac{1}{h} + \frac{1}{q_e} t$$

CHAPTER 4. RESULTS AND DISCUSSION

4.1. FTIR Analysis

FTIR spectra of MSSH and its associated activated carbons produced at 400 ℃ and 500 ℃ are shown in Fig. 3. Based on the results, noticeable changes can be seen between the precursor (MSSH) and the produced activated carbon. FTIR of the MSSH showed absorption peaks around 3305 cm^{-1} which is attributed to hydrogen-bonded O-H stretching, while the one observed at 2920 cm^{-1} can be assigned to unsymmetrical C–H stretching. The peaks at 1658 and 1512 cm^{-1} are due to the C=C stretching that can be assigned to the aromatic rings. FTIR spectrum of MSSH activated carbons prepared at 400 ℃ and 500 ℃ are almost the same. The carbon prepared at lower temperature showed a peak at 3355 cm^{-1} assigned to hydrogen-bonded O-H, while the absence of this peak in carbon prepared at 500 ℃, shows better dehydration during the production of AC. Other bands in AC-400 and AC-500, consist of peaks at around 1589 and 1581 cm^{-1}, respectively, indicating C=C stretching in aromatic rings.

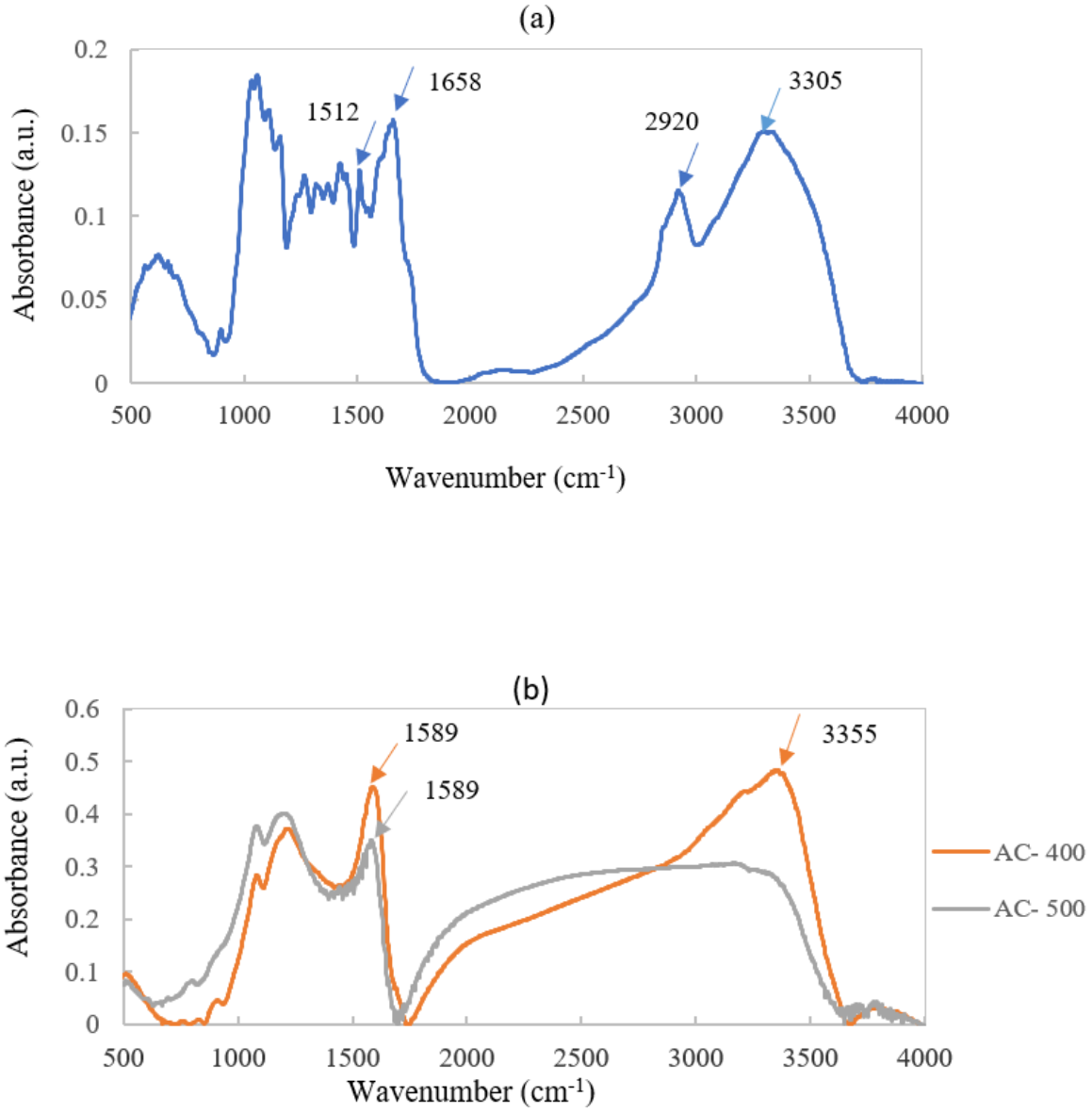

Fig. 3. Fourier transform infrared spectroscopy (FTIR) spectra for (a) MSSH and (b) Activated carbons prepared at 400 ℃ and 500 ℃.

4.2. Adsorbent properties

Fig. 4 shows the nitrogen adsorption-desorption isotherms of the ACs, and Table 3 summarizes the physical properties of the AC samples. Considering the International Union of Pure and Applied Chemistry (IUPAC) classification, both ACs showed type IV isotherms corresponding to hysteresis loop and mesoporous solid. Furthermore, given pore size distribution in Fig. 5 and average pore diameters in Table 3, both ACs identified as mesoporous, since IUPAC classified pore distribution based on the pore diameter (d) to microporous (d < 2 mm), mesoporous (d = 2-50) and microporous (d > 50 nm) (Rouquerol et al. 1994). As it can be seen in Table 3, the ACs also have micropore specific surface areas around 44% to 50% of the total BET specific surface area. The simultaneous formation of micropores and mesopores was also reported in previous studies (Benadjemia et al. 2011; Mahamad et al. 2015).

Based on the physical properties of AC samples (Table 3), it can be seen that the yield of both samples is in an acceptable range since a maximum 48% yield is expected to obtain for lignocellulosic precursors undergoing pyrolysis (Marsh and Reinoso, 2006).

Regarding the BET surface area, values obtained in this study are relatively large compared with those previously reported in the literature for ACs derived from lignocellulosic precursors (González-García 2018). Based on the result, AC prepared at higher carbonization temperature, i.e., 500 ℃, has a higher total pore volume and BET surface area. This can be due to the production of more pyrolytic vapors at higher temperatures which results in the formation of more pores in AC structure (Bertero et al. 2011; Ahmad and Alrozi 2011). Furthermore, aromatization enhanced in high carbonization temperature resulted in higher BET surface area (Smith et al. 2009). Hence, the sample carbonized at 500 ℃ is selected for the adsorption studies.

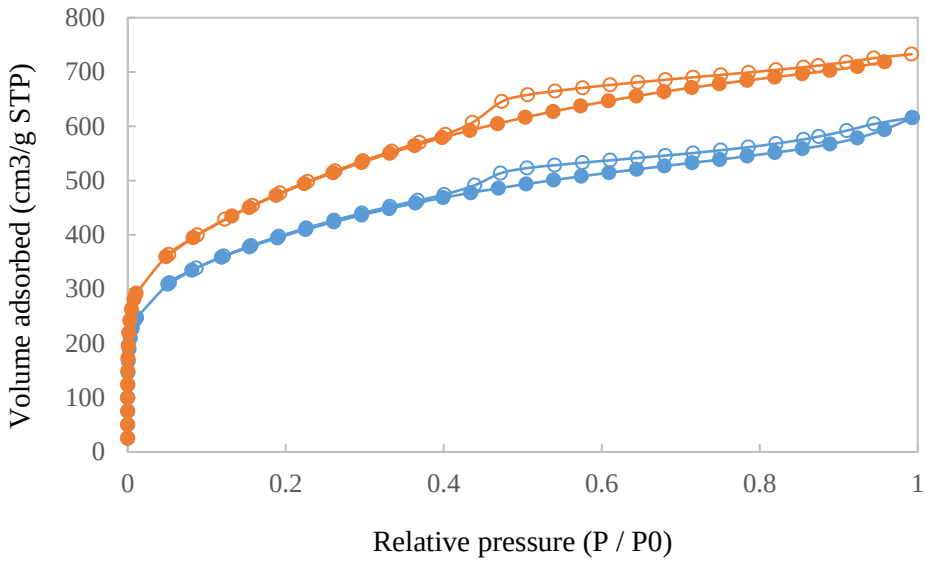

Fig. 4. Nitrogen adsorption-desorption isotherms of the activated carbons produced at 400 ℃ (blue circle) and 500 ℃ (orange circle).

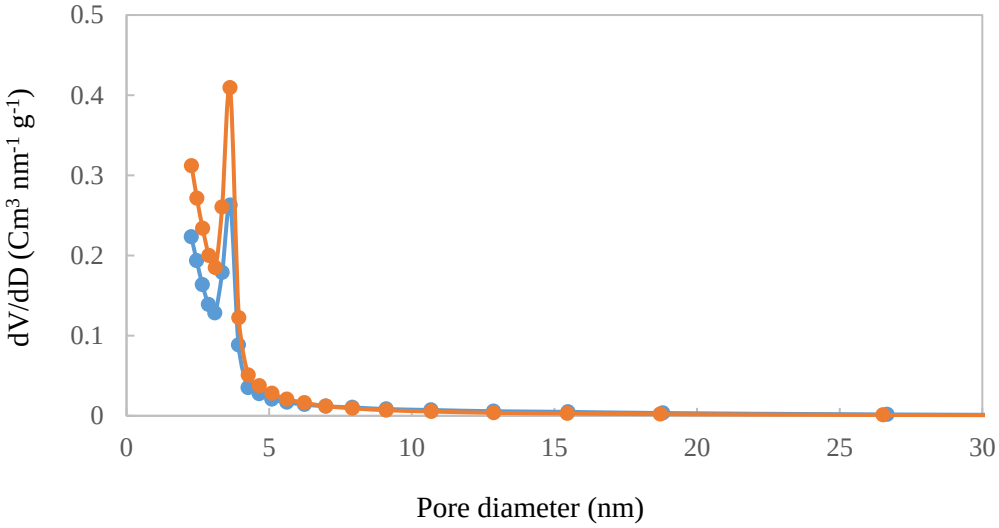

Fig. 5. Pore size distributions obtained by the BJH method of activated carbons produced at 400 ℃ (blue circle) and 500 ℃ (orange circle).

Table 3. Physical properties of activated carbons prepared from MSSH

Parameter	Activated Carbon Sample	
	AC-400	AC-500
Particle size (um)	250	250
Yield (%)	46.80	40.65
Burn off (%)	53.20	59.35
BET surface area (m^2/g)	1389	1693
Micropore surface area (m^2/g)	727	753
External surface area (m^2/g)	662	940
Total pore volume (cm^3/g)	0.95	1.13
Micropore volume (cm^3/g)	0.33	0.33
Mesopore volume (cm^3/g)	0.62	0.80
Average pore diameter (nm)	2.7	2.6

4.3. Batch adsorption studies

4.3.1. Effect of pH

The effect of pH on the adsorption of RB5 and BB3 onto the AC is shown in Fig. 6. After 2 hours, the amount of RB5 removal decreased from 99.5 % to 62.2 % as pH increased from 2 to 4, respectively, and then remained almost constant. This shows the amphoteric character of AC that its surface charge might be positive or negative, considering the pH of the solution. At pH < pH_{pzc}, the charge of AC surface would be positive, favoring the adsorption of anionic species due to high electrostatic attraction. By contrast, adsorption of cationic species will increase at pH > pHpzc, where the charge of carbon surface is negative (Rodriguez-Reinoso 1998). In this study, the pHpzc of the prepared AC is 4 (Fig. 7), thus higher removal of RB5 as an anionic dye is expected in pH < 4. By contrast, the removal of BB3 as a cationic dye is expected to be higher in pH > 4. Although after 2 hours, this trend was observed, in both dye solutions, after 24 hours

monitoring period, when the equilibrium was reached, almost 100% dye was adsorbed on AC regardless of solution pH. This means that electrostatic interactions between the functional groups of AC and dyes were not the primary adsorption mechanism. Another possible mechanism that can be considered is chemisorption, which is the chemical reaction between the dyes and the AC. So based on the solution pH, the adsorption can occur through either electrostatic attraction or non-electrostatic interaction, such as p-p interaction, hydrogen bonding, and electron donor-acceptor complex mechanism (Moreno-Castilla 2004). Similar observations were found in the adsorption of Congo Red (Namasivayam and Kavitha 2002) and Acid Violet (Namasivayam et al. 2001) on AC prepared from coir pith. Their results showed that dye removal decreased slightly when the pH increased from 2 to 4 and then remained almost constant up to pH 10.

Furthermore, it can be seen that at the same initial concentration and pH, after 2 hours contact time, the removal of BB3 is higher than RB5, although a much smaller amount of AC was applied for BB3 removal. This shows that the prepared AC has much more affinity towards cationic dyes than an anionic one, most probably due to its low pHpzc resulting from the acidic oxygenated groups on its surface.

Based on the results, since the change in solution pH does not significantly change the prepared activated carbon's performance at equilibrium, the rest of the experiments were done without any pH adjustment and at the initial pH of RB5 and BB3 aqueous solutions which is 6 and 6.2 respectively.

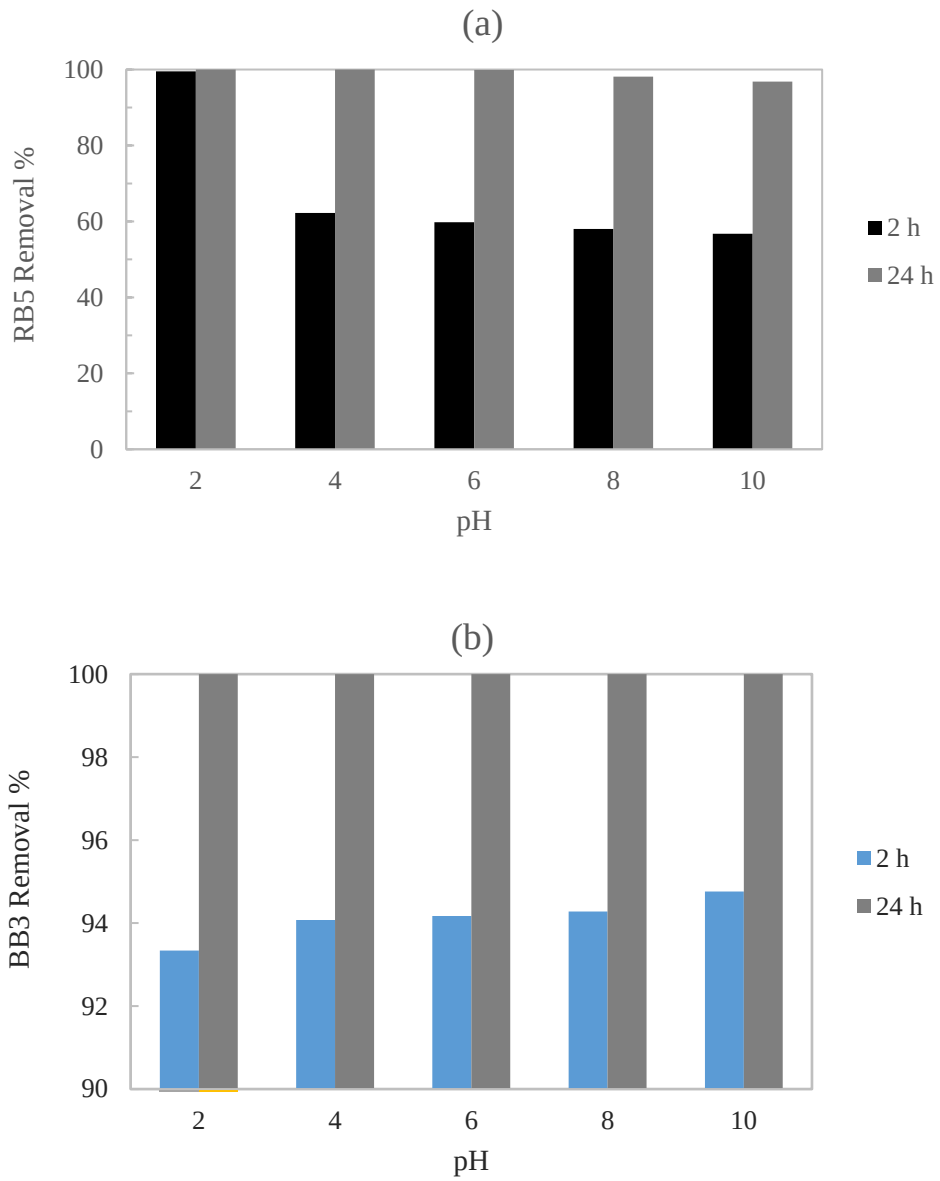

Fig. 6. Effect of pH on adsorption of (a) RB5 and (b) BB3 onto MSSH activated carbon

(Experimental conditions: temperature = 30 ℃; dye concentration: 50 mg/L; AC dosage: 2 g/L and 0.1 g/L for RB and BB3, respectively).

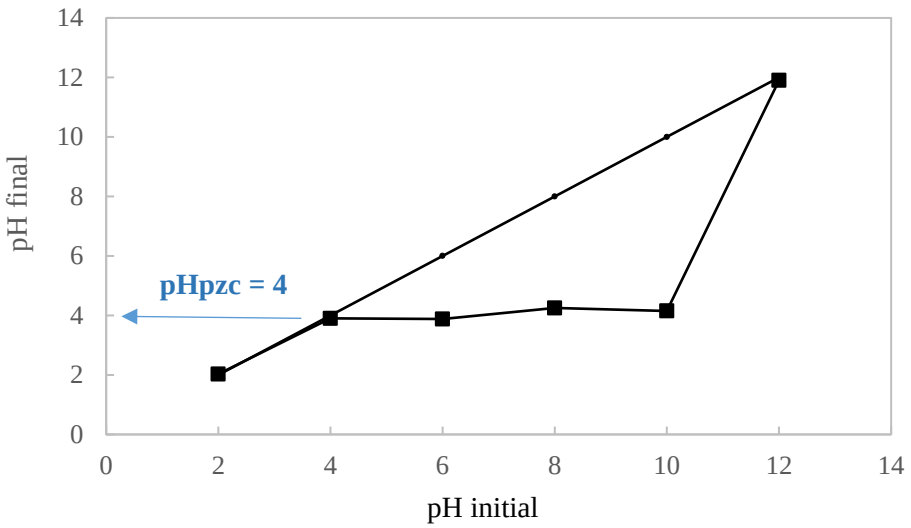

Fig. 7. Determination of pH_{pzc} of activated carbon produced from MSSH

4.3.2. Effect of contact time

To investigate the effect of contact time on the amount of adsorbed dye, batch adsorption experiments for RB5 and BB3 were carried out at the initial dyes' concentration of 50, 100, and 150 mg/L and different time intervals (Fig. 8). It was found that the amount of adsorbed BB3 and RB5 on the AC increased as the contact time increased until the equilibrium was reached. A significant amount of BB3 (80.5%) was removed after 30 minutes when the dye concentration was 50 mg/L, and afterward, the adsorption rate became slow. This trend was also observed for initial BB3 concentrations of 100 and 150 mg/L, where 65.7% and 46.1% were removed after 30 minutes, respectively. The equilibrium time for BB3 was found to be 1 hour for concentration of 50-150 mg/L. Hameed and Duad (2008) reported a similar trend in the adsorption of BB3 on AC prepared from *Hevea brasiliensis* seed coat. Their results showed that BB3 removal occurred very fast at the beginning and after 1 hour reached an equilibrium.

Rapid adsorption at the primary stage is due to the presence of more available sites on the surface of AC at the initial phase of the adsorption process. As the sites are occupied by dye molecules, the electrostatic repulsion between the species that are adsorbed on the surface of ACs and those that remain in the solution causes the adsorption rate to become slower. Moreover, the pore diffusion of the solute into the porous structure of the AC occurs slowly, which results in a slow rate of the adsorption process.

A similar trend was observed for RB5 removal; however, longer contact time (24 hours) was required for the maximum removal of RB5, which is 99.7%, 80.7, and 66.3% for RB5 initial concentration of 50, 100, and 150 mg/L, respectively. The same trend was found in the study of Felista et al. (2020) for the adsorption of RB5 using macadamia seed Husks.

For BB3, the equilibrium time was found to be nearly 1 hour when 94.3%, 77%, and 57% of BB3 were removed with initial concentrations of 50, 100, and 150 mg/L, respectively. However, after 24 hours monitoring period still, a slight increase in BB3 removal was noticed, and the maximum removal was reported to be 99.7, 81.4, and 62.7%, respectively. As a result, equilibrium time was conservatively considered to be 24 hours for subsequent adsorption experiments of both dyes to standardize the experimental condition.

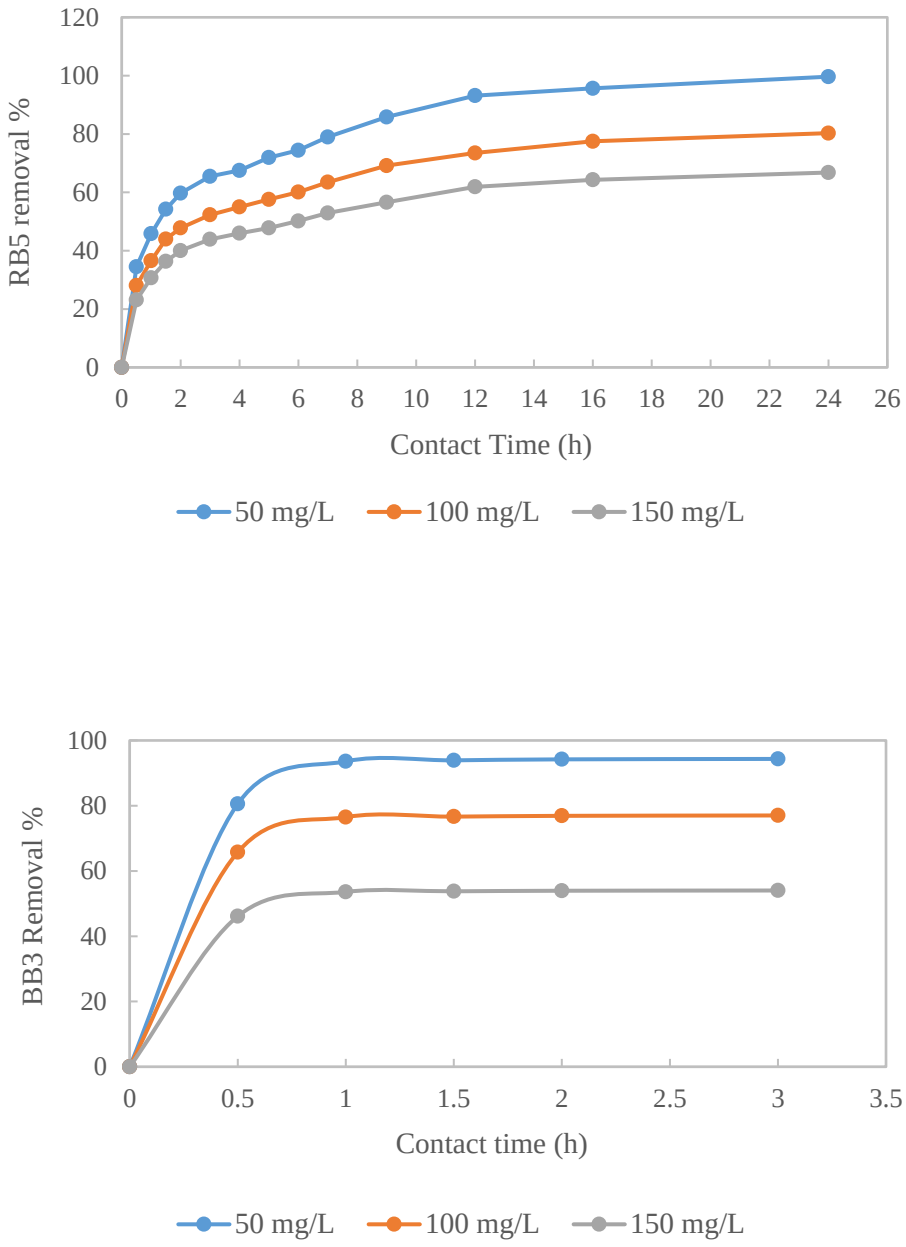

Fig. 8. Effect of contact time on adsorption of RB5 and BB3 onto MSSH activated carbon (AC dosage: 2 and 0.1 g/L for RB and BB3, respectively).

4.3.3. Effect of adsorbent dosage

A given quantity of activated carbon is able to adsorb only a specific amount of adsorbate. Therefore, the initial adsorbent dosage is of great importance. In this study, to investigate the effect of AC dosage on dye removal, 50 mL of dye solutions with an initial dye concentration of 50, 100, and 150 mg/L were mixed with different dosages of AC for 24 hours using jar test at 30 °C (Fig. 9). It can be seen that as the AC dosage increased, the dye removal percentage also increased until it reached a constant value. This is because a higher amount of AC provides more active surface sites for adsorbing dye molecules, and when all sites are occupied with adsorbate species, no more adsorption occurs. Previous studies also reported higher dye removal with increasing the AC dosage (Gong et al. 2005; Namasivayam and Kavitha 2002; Mahmoodi et al. 2011).

Optimum adsorbent dosage for RB5 and BB3 removal was found to be 2 g/L and 0.1 g/L of AC for 50 mL of 50 mg/L dye solution, respectively. For the initial concentrations of 100 and 150 mg/L, the optimum AC dosage for RB5 would be 3 g/L, and for BB3 would be 0.2 and 0.3 g/L, respectively.

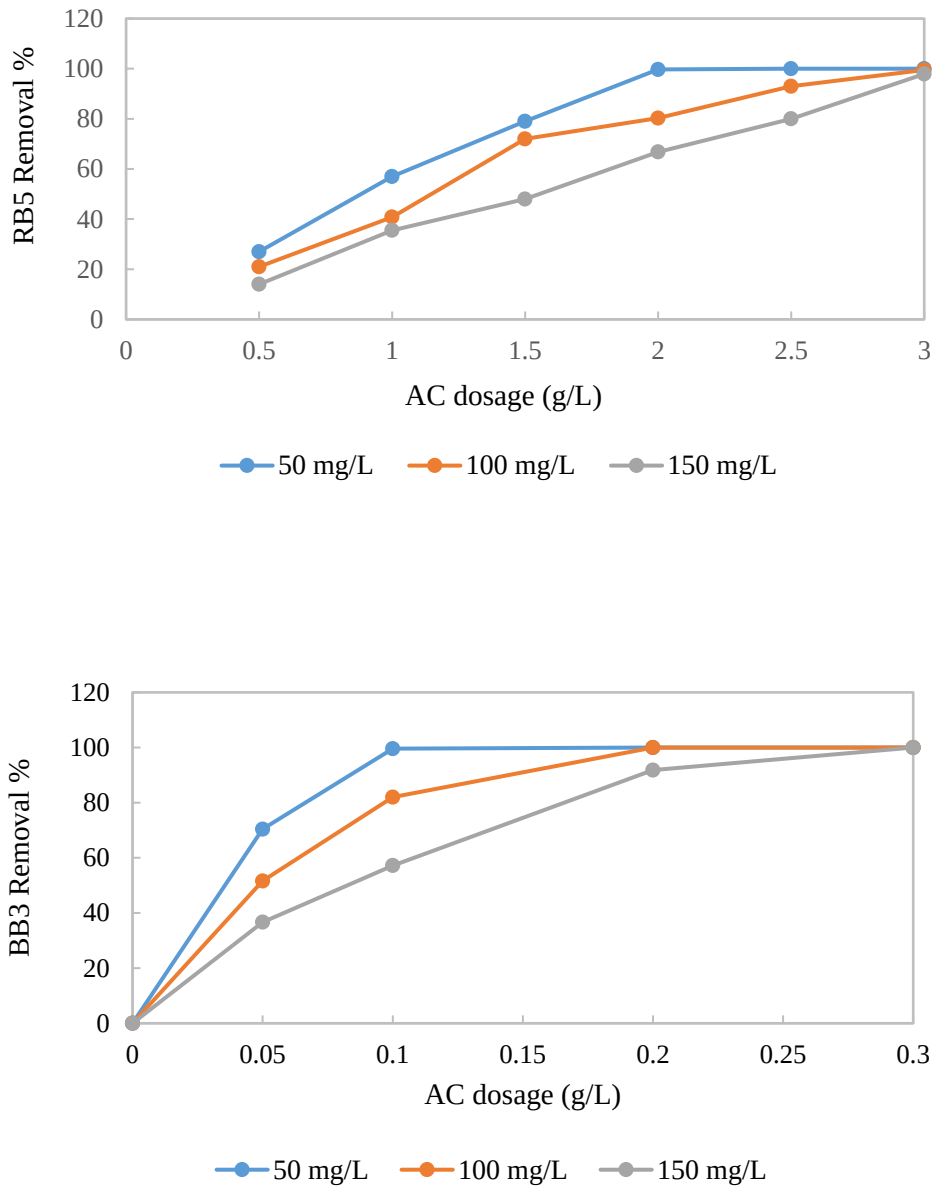

Fig. 9. Effect of AC dosage on adsorption of RB5 and BB3 onto MSSH activated carbon

4.3.4. Effect of initial dye concentration

The effects of initial dye concentration on the percentage of dye removal were studied. Three different doses of AC were added to 50 mL solutions with different dye concentration between 50 and 200 mg/L. It was noticed that for both dyes, increasing initial dye concentration resulted in a decrease in dye removal percentage, as illustrated in Fig. 10. When the dye concentration is lower, the number of dye moles compared to the available sites on the surface of AC is also lower. While when the dye concentration is high, the number of dye moles can be more than the available adsorption sites. As a result, for a specific dosage of AC, the amount of dye removal depends on the dye initial concentration.

This result is in compliance with previous studies on adsorption of anionic dye using AC from orange peel (Khaled et al. 2009), and cationic dyes using peanut hull (Gong et al. 2005), where the dyes' removal percentage were greater at lower initial concentrations and smaller at higher initial concentrations.

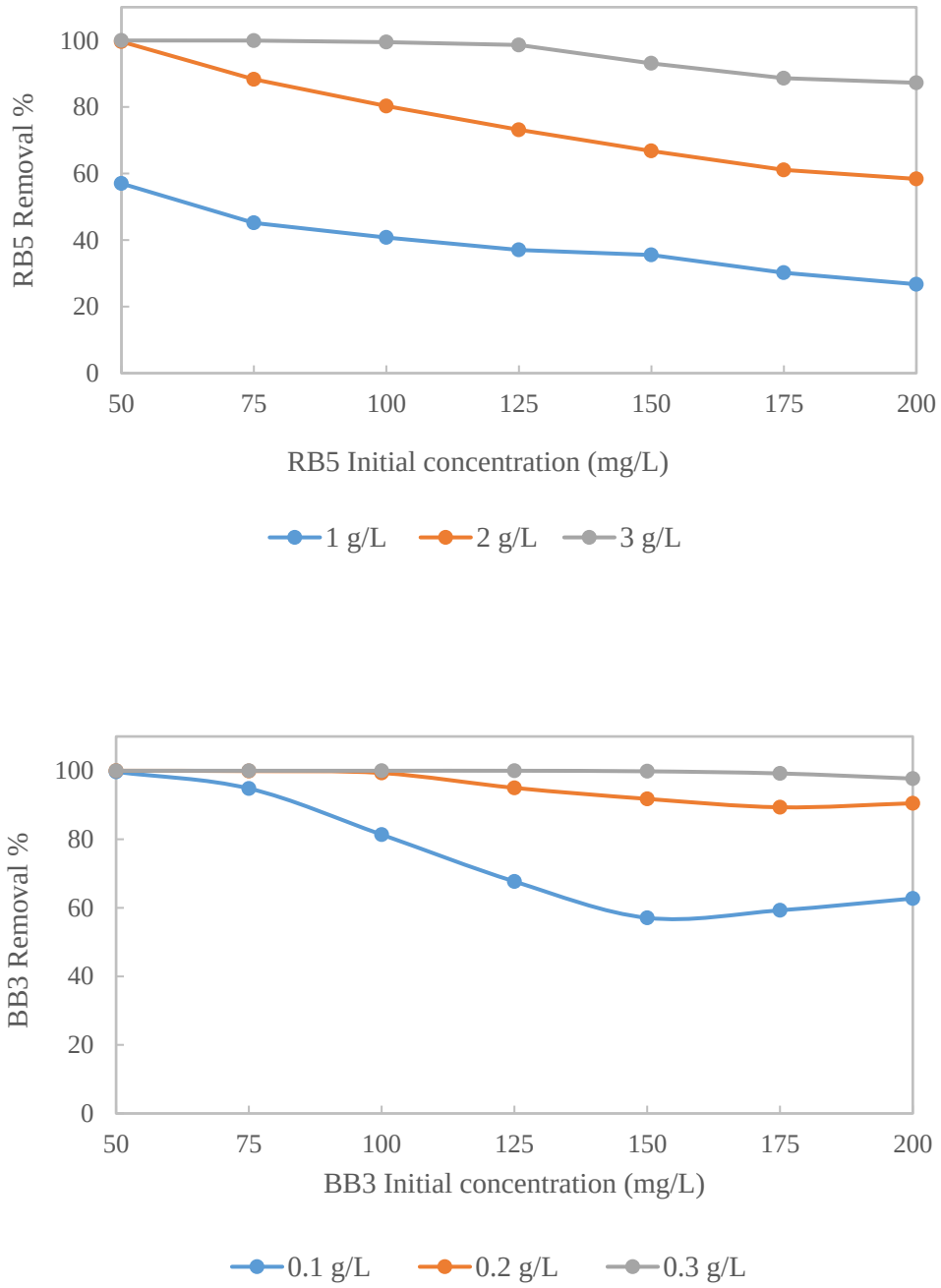

Fig. 10. Effect of initial dye concentration on adsorption of RB5 and BB3 onto MSSH activated carbon.

4.4. Adsorption isotherm models

The equilibrium data of RB5 and BB3 adsorption onto MSSH activated carbon was fitted with Langmuir and Freundlich isotherm plots (Fig. 11-14). Isotherm parameters were calculated and summarized in Table 4. It can be seen that correlation coefficients, is high for the Langmuir isotherm model ($R^2 > 0.98$) compared to the Freundlich model ($R^2 < 0.98$), which implies that the adsorption of anionic dye (RB5) and cationic dye (BB3) on the produced AC follows the Langmuir isotherm model. Furthermore, the value of separation factor (R_L), which is in the range of 0-1, indicates the favorability of dye adsorption on the produced AC. Thus, according to the assumption of the Langmuir model, the dye uptake by the AC continues until a monolayer coverage of dye molecules is formed onto the homogeneous surface of the AC, and no more adsorption occurs at the occupied sites. The maximum monolayer adsorption capacity calculated from the Langmuir isotherm model was 833.33 and 67.11 mg/g for adsorption of BB3 and RB5, respectively. These amounts are relatively close to those obtained from experiments, which are 856.2 and 58.4 mg/g, respectively, which indicates that the Langmuir isotherm model can appropriately describe the adsorption process of RB5 and BB3 on to the surface of produced AC.

Table 4. The Langmuir and Freundlich isotherm parameters for the adsorption of RB5 and BB3 dye onto MSSH activated carbon

Dye	AC conc. (g/L)	Langmuir Isotherm model				Freundlich Isotherm model			
		Q_m (mg/g)	K_L (L/mg)	R_L	R^2	1/n	n	K_F (mg/mg)(L/mg)$^{1/n}$	R^2
RB5	1	67.11	0.029	0.1459	0.9852	0.3644	2.74	7.97	0.9594
	2	63.69	0.089	0.0530	0.9913	0.1326	7.54	23.60	0.9038
BB3	0.1	833.33	1.500	0.0033	0.9998	0.0929	10.76	124.88	0.9797
	0.2	769.23	1.857	0.0027	0.9878	0.1225	8.16	116.75	0.9682

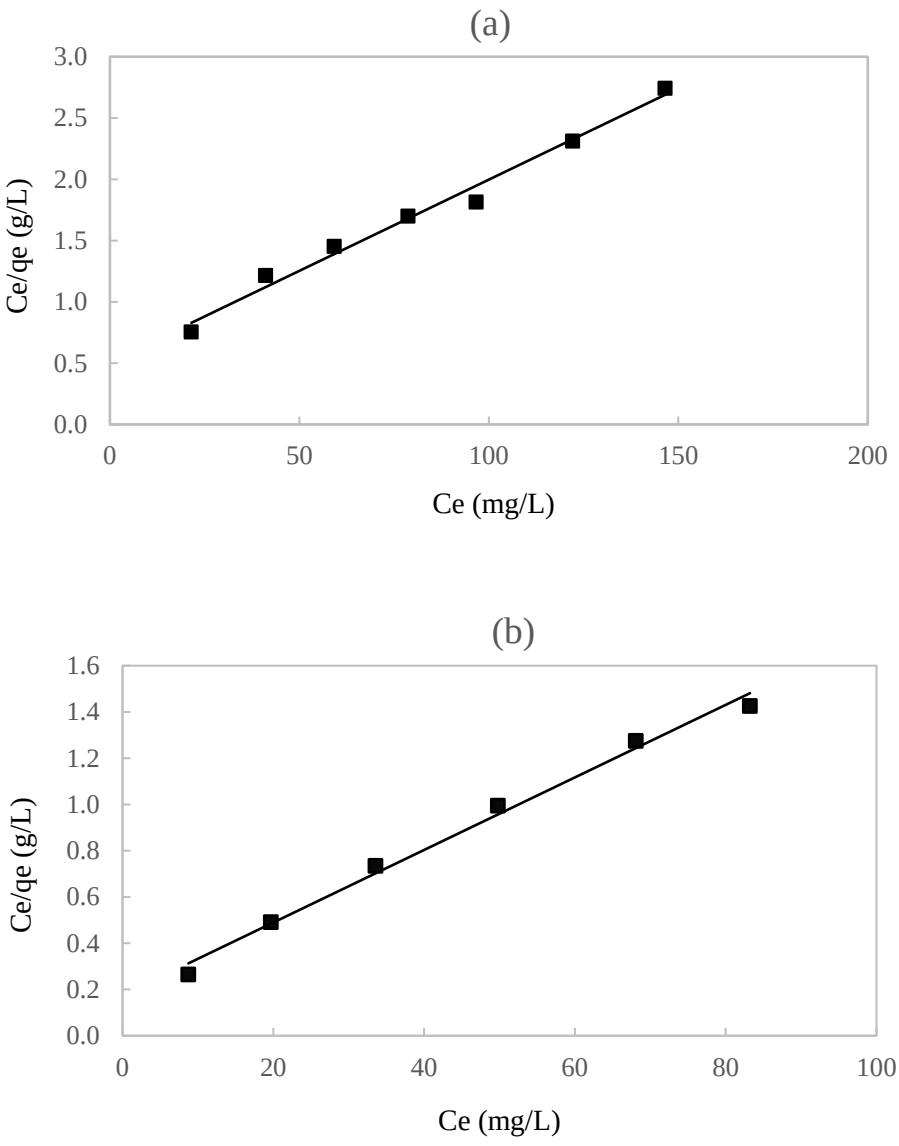

Fig. 11. Langmuir isotherms plots for anionic RB5 adsorption by MSSH activated carbon. (AC dosage: (a): 1 g/L and (b): 2 g/L).

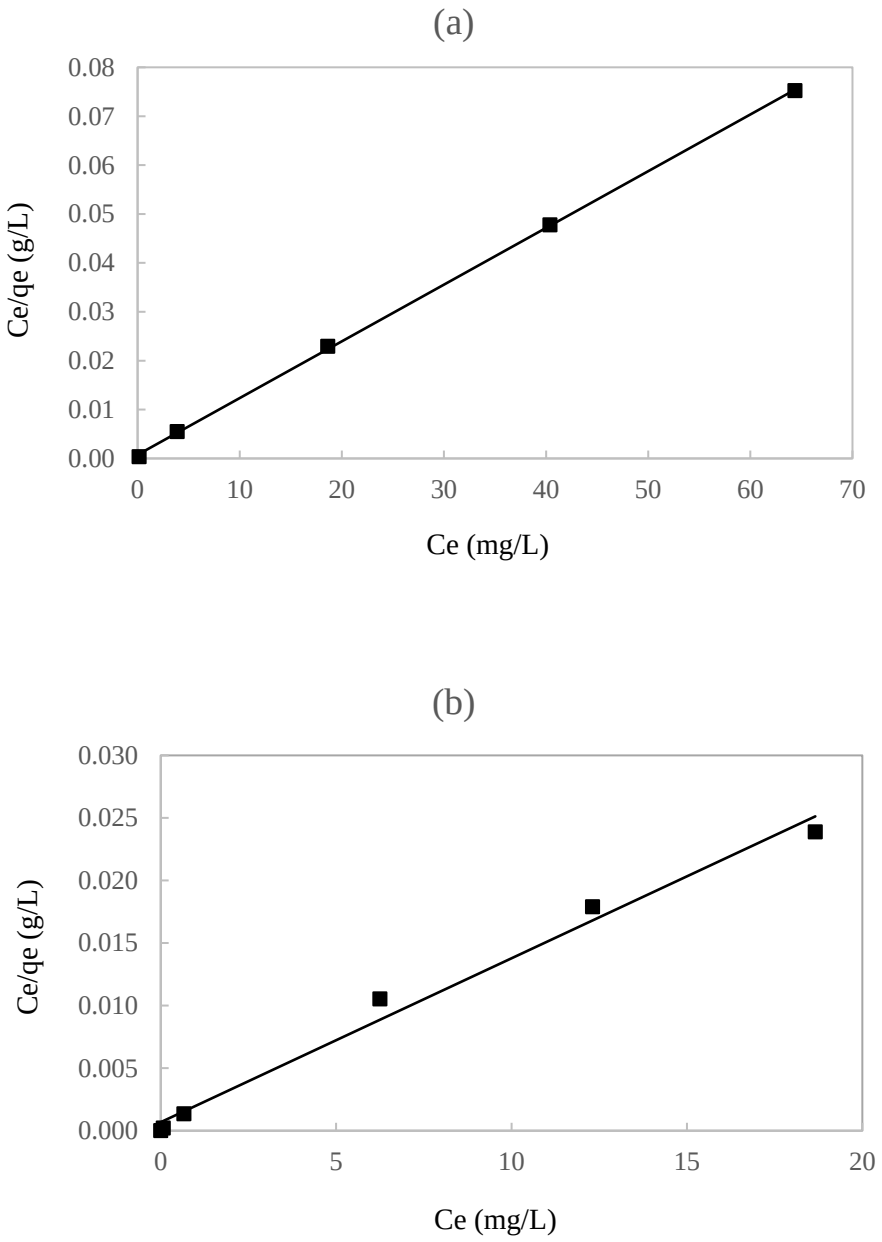

Fig. 12. Langmuir isotherms plots for cationic BB3 adsorption by MSSH activated carbon. (AC dosage: (a): 0.1 g/L and (b): 0.2 g/L).

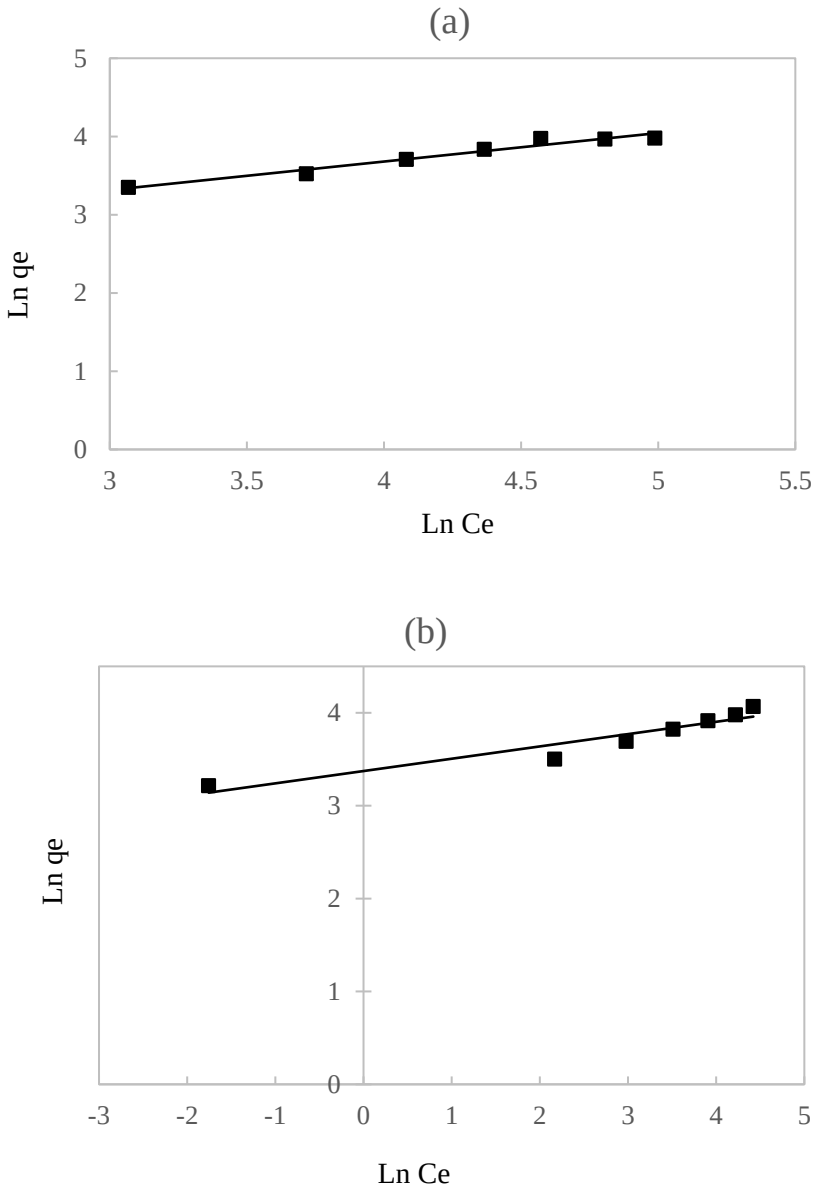

Fig. 13. Freundlich isotherms plots for anionic RB5 adsorption by MSSH activated carbon. (AC dosage: (a): 1 g/L and (b): 2 g/L).

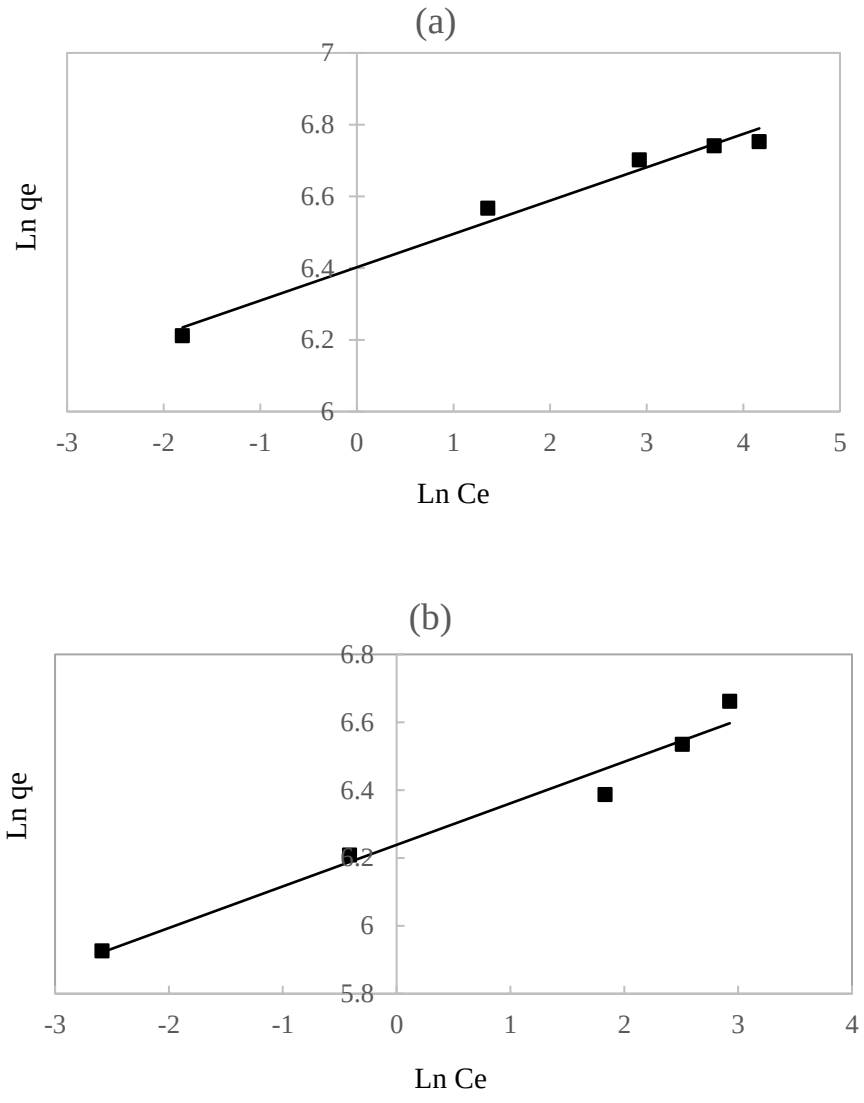

Fig. 14. Freundlich isotherms plots for cationic BB3 adsorption by MSSH activated carbon. (AC dosage: (a): 0.1 g/L and (b): 0.2 g/L).

4.5. Adsorption kinetic study

The pseudo-first order and pseudo-second-order kinetic models for RB5 and BB3 dye adsorption onto the MSSH activated carbon were plotted and shown in Fig. 15 and 16. The models' properties were calculated and summarized in Table 5. It can be seen that at all dye concentrations,

the correlation coefficients of pseudo-second order are near to 1, and higher than the R^2 values of the pseudo-first-order kinetic model. Furthermore, the adsorptive capacities calculated from the pseudo-second-order kinetic model are much closer to the experimental data. Therefore, adsorption of RB5 and BB3 on the produced AC follow the pseudo-second-order kinetic model, which implies that the chemical adsorption or chemisorption is probably the phenomenon that controls the rate of adsorption through valency forces arising from sharing or exchange of electrons between AC and dyes. A similar result was found in the adsorption of Basic Blue 3 on AC prepared from rubber seed coat (Hameed and Daud, 2008) and adsorption of Direct N Blue-106 on AC prepared from orange peel (Kaled et al., 2009).

Table 5. Kinetic parameter of the pseudo-first order and pseudo-second-order for the adsorption of RB5 and BB3 dyes.

Dye	Dye conc. (mg/L)	q_e (exp.)	Pseudo-first-order kinetic model			Pseudo-second-order kinetic model		
		mg/g	k_1 (h^{-1})	q_e cal (mg/g)	R^2	k_2 (g/(mg h))	q_e cal (mg/g)	R^2
RB5	50	24.91	0.222	15.35	0.967	0.0211	26.39	0.995
	100	40.15	0.175	25.76	0.987	0.0131	42.55	0.993
	150	58.40	0.171	32.14	0.986	0.0105	53.19	0.995
BB3	50	498.35	0.047	152.26	0.960	0.0005	476.19	0.999
	100	813.66	0.048	266.50	0.962	0.0003	769.23	0.999
	150	856.20	0.052	359.50	0.965	0.0002	833.33	0.999

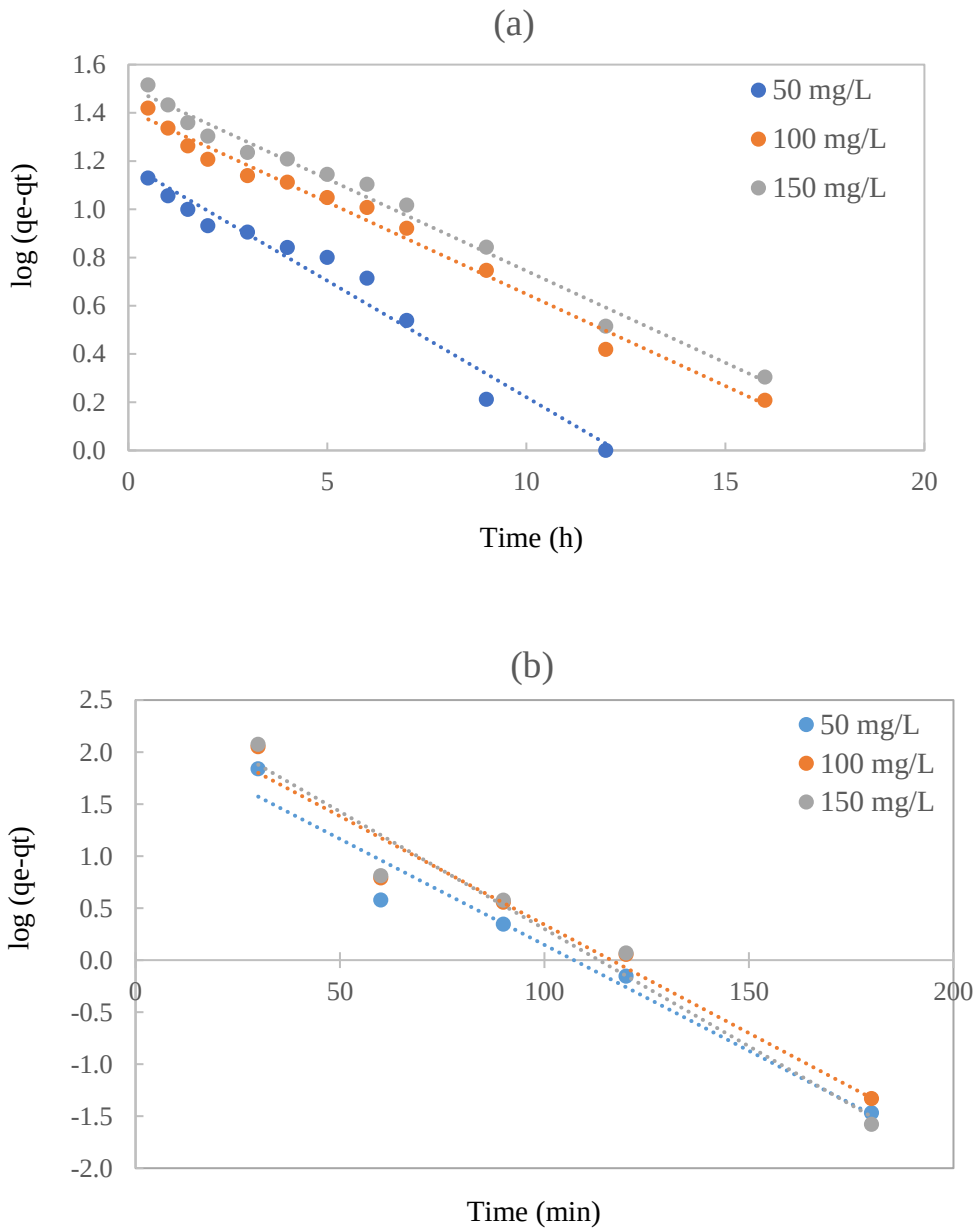

Fig. 15. Plots of the pseudo-first-order kinetic model for adsorption of (a) RB5 and (b) BB3.

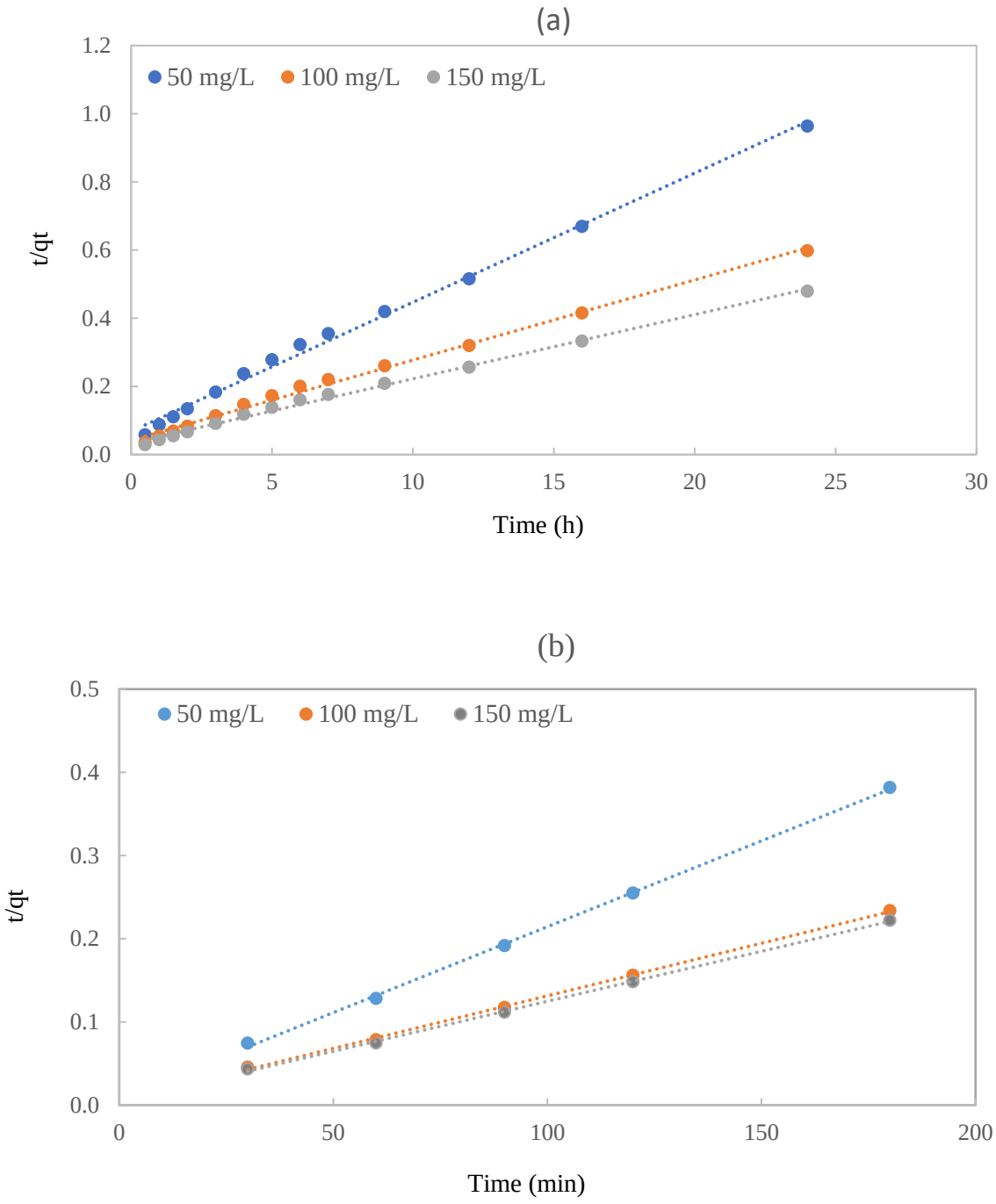

Fig. 16. Plots of the pseudo-second-order kinetic model for adsorption of (a) RB5 and (b) BB3.

4.6. Dye adsorption in synthetic textile wastewater

To investigate the performance of produced AC in textile wastewater, which contains a mixture of different dyes and other organic and inorganic additives, simulated textile wastewater containing both RB5 and BB3 was prepared based on Table 2. Fig. 17 shows the performance of AC in distilled water and synthetic textile wastewater. As mentioned before, the required amount of AC for complete removal of 100 mg/L RB5 and BB3 dye solution is 3 g/L and 0.2 g/L, respectively. As a result, for a solution containing a mixture of these dyes, 3 g/L of AC was applied to ensure a satisfactory removal of both dyes. By comparing Fig. 17, a, and b, it can be seen that 100% BB3 removal was achieved in both distilled water and synthetic textile wastewater. Regarding the anionic dye, RB5, although it was removed almost 100% in both solutions; the complete removal took around 1 hour in textile wastewater while it took almost 24 hours in distilled water. The higher dye removal efficiency in textile wastewater is due to the presence of salt ions, which can induce the aggregation of dye molecules and increase the amount of dye adsorbed on the AC surface (Mishra 2020). This result is in agreement with the study of Khaled et al. (2009) who reported a 5 percent increase in DNB-106 removal from synthetic textile wastewater compared to distilled water.

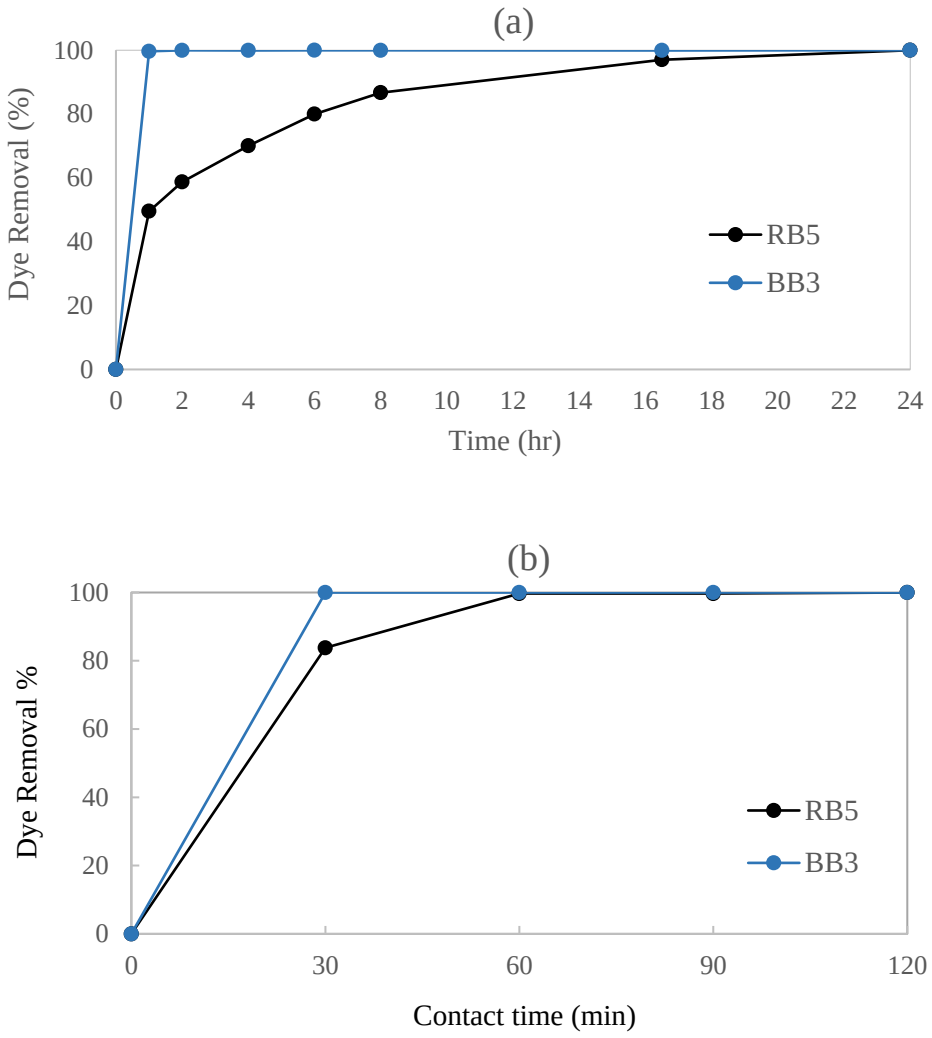

Fig. 17. Percentage of dye removal in (a) distilled water and (b) synthetic textile wastewater. RB5 concentration:100 mg/L, BB3 concentration: 100 mg/L, AC dosage: 3 g/L, pH:6.

4.7. Comparison with commercial activated carbon

To compare the performance of produced AC with the ACs that are commercially available, powdered AC treated with phosphoric acid and sulfuric acid was purchased from Sigma-Aldrich. We wanted to find the AC doses that are required for complete dye removal from synthetic

textile wastewater in 1 hour contact time which is usually considered as a common contact time in large-scale applications.

Fig. 18 shows the percentage of dye removal from synthetic textile wastewater with the commercial AC. Comparing this figure with Fig. 17 (b) indicates that both ACs are capable of removing almost 100 % of dyes in 1 hour. However, this high removal percentage was achieved with 3 g/L of AC produced in this study and with 1 g/L of commercial AC.

Although the amount of AC dosage required for 100% removal is lower with commercial AC, its production cost should be investigated compared to the MSSH activated carbon, which is made from an inexpensive and widely available precursor. Moreover, using only phosphoric acid with a low concentration as an impregnation agent in producing MSSH activated carbon can make it a better option compared to the commercial one that applied different impregnating chemicals, i.e., sulfuric acid and phosphoric acid, to produce AC.

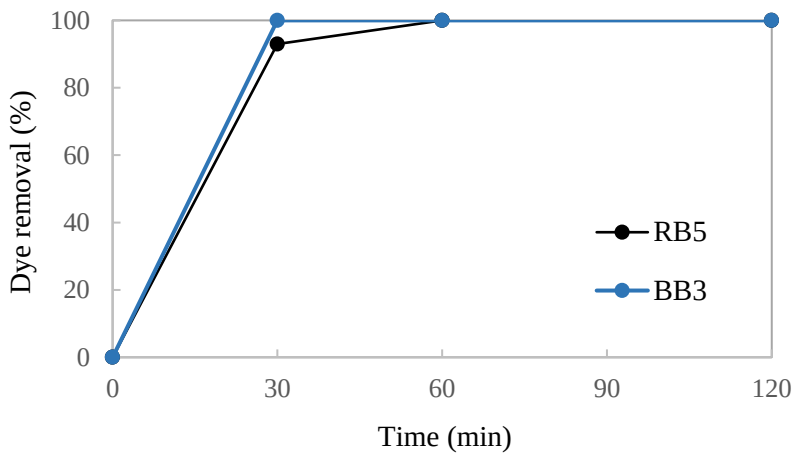

Fig. 18. Percentage of dye removal in synthetic textile wastewater with commercial activated carbon. RB5 concentration:100 mg/L, BB3 concentration: 100 mg/L, AC dosage: 1 g/L, pH:6.

CHAPTER 5. CONCLUSION

This research focused on the MSSH potential for activated carbon production since no work has been done on it so far. Impregnating the precursor with phosphoric acid at a 1:3 ratio followed by pyrolysis at 500 ℃ resulted in AC with a higher BET surface area (1693 m^2/g) compared to the one activated at 400 ℃ (1389 m^2/g), thus the former was selected for the rest of the experiments. Adsorption batch tests showed that dye removal could be significant in the original pH of dye solutions which was around 6. It was also found that the percentage of dye removal increased with increasing contact time and adsorbent dosage up to a certain point and remained constant thereafter. However, the amount of dye adsorbed on the AC decreased by increasing the initial dye concentration.

Isotherm studies showed that the adsorption behavior of MSSH activated carbon can be described by a monolayer Langmuir isotherm. The maximum monolayer adsorption capacity of prepared AC is 833 and 67 mg/g for BB3 and RB5, respectively, which shows that the MSSH activated carbon has a higher affinity toward cationic dyes than anionic dyes, most probably because of its surface acidity. The kinetic modeling of the adsorption of the dyes onto the AC well followed the pseudo-second-order rate model with correlation coefficients as high as 0.99.

Results also showed that the produced AC can be considered as a highly efficient adsorbent for treating textile wastewater, containing a mixture of dyes, i.e., RB5 and BB3. 100% dye removal was achieved in one hour, at pH 6, by applying 3 g/L activated carbon at 30 ℃ when the concentration of each dye was as high as 100 mg/L.

Adsorption studies with commercial AC revealed that the AC produced in this study can be competitive to the commercial one considering its high removal efficiency and low-cost production.

According to this study diverting the seed husk of *M. Stenopetala* from disposal and converting it to a valuable product, i.e., activated could be a sustainable and economic option for textile wastewater treatment. As this research is the first one studying the potential of MSSH to produce AC, more investigation is needed to improve the production method and obtain a higher surface area. Furthermore, considering the large-scale application, the AC production cost, and the feasibility of AC regeneration after the treatment process need to be investigated.

CHAPTER 6. ENGINEERING SIGNIFICANCE

The findings of this study will redound to the benefit of the environment considering that efficient organic waste management and diversion from landfills play an important role in protecting the environment. Agricultural waste constitutes a huge amount of organic waste that can be converted to valuable products as a promising alternative to landfill disposal. One of the high-value-added products suitable for a wide range of pollutant remediation is activated carbon. A lot of research has been done so far on activated carbon production from agricultural waste and its applicability for different purposes. However, no work has been reported previously on the potential of *M. stenopetala* seed husks for activated carbon production.

This study managed *M. stenopetala* seed husk, as a biomass and utilized it in an efficient and economical way to produce high porous activated carbon. Hence, waste will be converted to a valuable and versatile product, i.e., activated carbon that can be applied to remove different pollutants from different sources. Among its various applications, this study showed that the produced waste-derived activated carbon can totally remove dyes from colored effluent, i.e., textile wastewater, which if not properly treated, negatively affects the receiving water bodies and the environment mainly due to the dyes' toxic nature.

Furthermore, from the academic perspective, this study will help the researchers uncover critical areas in making activated carbon from *M. stenopetala* seed husks, particularly in terms of optimum conditions since no research have been investigated on it so far.

REFERENCES

Abdullah, Nor Salmi, Mohd Hazwan Hussin, Syazrin Syima Sharifuddin, and Muhammad Azroie Mohamed Yusoff. 2017. 'Preparation and characterization of activated carbon from moringa oleifera seed pod', Cellulose, 28: 0.50.

Abiyu, Asaminew, Denghua Yan, Abel Girma, Xinshan Song, and Hao Wang. 2018. 'Wastewater treatment potential of Moringa stenopetala over Moringa olifera as a natural coagulant, antimicrobial agent and heavy metal removals', Cogent Environmental Science, 4: 1433507.

Agency, US Environmental Protection. 1996. 'Best management practices for pollution prevention in the textile industry'.

Ahmad, Mohd Azmier, and Rasyidah Alrozi. 2011. 'Removal of malachite green dye from aqueous solution using rambutan peel-based activated carbon: Equilibrium, kinetic and thermodynamic studies', Chemical Engineering Journal, 171: 510-16.

Ahmed, T, SI Promi, and IJ Rumpa. 2018. "Color Removal from Tannery Wastewater Using Activated Carbon Generated from Rice Husk." In World Environmental and Water Resources Congress 2018: Water, Wastewater, and Stormwater; Urban Watershed Management; Municipal Water Infrastructure; and Desalination and Water Reuse, 312-21. American Society of Civil Engineers Reston, VA.

Al-Kdasi, Adel, Azni Idris, Katayon Saed, and Chuah Teong Guan. 2004. 'Treatment of textile wastewater by advanced oxidation processes—a review', Global nest: the Int. J, 6: 222-30.

Babu, B Ramesh, and AK Parande. 'Raghu, & Kumar, TP (2007). Cotton textile processing: waste generation and effluent treatment', The Journal of Cotton Science, 11: 110-22.

Banerjee, Sushmita, and MC Chattopadhyaya. 2017. 'Adsorption characteristics for the removal of a toxic dye, tartrazine from aqueous solutions by a low cost agricultural by-product', Arabian Journal of Chemistry, 10: S1629-S38.

Benadjemia, Millière, L. Millière, L. Reinert, N. Benderdouche, and L. Duclaux. 2011. "Preparation, characterization and Methylene Blue adsorption of phosphoric acid activated carbons from globe artichoke leaves." Fuel Processing Technology 92, no. 6: 1203-1212.

Benefield, LD, JF Judkins, and BL Weand. 1982. 'Fundamentals of surface and colloidal chemistry', Process Chemistry for Water and Waste Water Treatment, Benefield, LD, JK Judkins and BL Weand (Eds.). Prentice Hall, Inc., Englewood Cliffs, NJ: 191-210.

Bertero, Melisa, Gabriela de la Puente, and Ulises Sedran. 2011. "Effect of pyrolysis temperature and thermal conditioning on the coke-forming potential of bio-oils." Energy & Fuels 25, no. 3: 1267-1275.

Bhatnagar, Amit, William Hogland, Marcia Marques, and Mika Sillanpää. 2013. 'An overview of the modification methods of activated carbon for its water treatment applications', Chemical Engineering Journal, 219: 499-511.

Boeniger, MF. 1980. 'Carcinogenity of azo dyes derived from benzidine', Department of Health and Human Services (NIOSH), Pub.

Burch, Paula. 2013. 'About Fiber Reactive Dyes', All About Hand Dyeing.

Cagnon, Benoît, Xavier Py, André Guillot, Fritz Stoeckli, and Gérard Chambat. 2009. 'Contributions of hemicellulose, cellulose and lignin to the mass and the porous properties of chars and steam activated carbons from various lignocellulosic precursors', Bioresource Technology, 100: 292-98.

Carr, Kathryn. 1995. 'Reactive dyes, especially bireactive molecules: structure and synthesis.' in, Modern Colorants: Synthesis and Structure (Springer).

Ching, Sim Lan, Mohd Suffian Yusoff, Hamidi Abdul Aziz, and Muhammad Umar. 2011. 'Influence of impregnation ratio on coffee ground activated carbon as landfill leachate adsorbent for removal of total iron and orthophosphate', Desalination, 279: 225-34.

Chowdhury, Shamik, Rahul Mishra, Papita Saha, and Praveen Kushwaha. 2011. 'Adsorption thermodynamics, kinetics and isosteric heat of adsorption of malachite green onto chemically modified rice husk', Desalination, 265: 159-68.

Chowdhury, Zaira Zaman, Sharifuddin Mohd Zain, Rashid Atta Khan, Rahman Faizur Rafique, and Khalisanni Khalid. 2012. 'Batch and fixed bed adsorption studies of lead (II) cations from aqueous solutions onto granular activated carbon derived from Mangostana garcinia shell', BioResources, 7: 2895-915.

Contescu, Cristian I, Shiba P Adhikari, Nidia C Gallego, Neal D Evans, and Bryan E Biss. 2018. 'Activated carbons derived from high-temperature pyrolysis of lignocellulosic biomass', C, 4: 51.

Council, National Research. 2006. Lost Crops of Africa: Volume II: Vegetables (National Academies Press).

Cox, PJ. 1995. "The kirk-othmer encyclopedia of chemical technology": Volume 10, Explosives and Propellants to Flame Retardants: JI Kroschwitz and M. Howe-Grant (editors), Wiley, New York.

Crini, Gregorio. 2006. 'Non-conventional low-cost adsorbents for dye removal: a review', Bioresource Technology, 97: 1061-85.

Crittenden, John C, R Rhodes Trussell, David W Hand, Kerry Howe, and George Tchobanoglous. 2012. MWH's water treatment: principles and design (John Wiley & Sons).

Danish, Mohammed, and Tanweer Ahmad. 2018. 'A review on utilization of wood biomass as a sustainable precursor for activated carbon production and application', Renewable and Sustainable Energy Reviews, 87: 1-21.

Degefu, Dagmawi Mulugeta, and Mekibib Dawit. 2013. 'Chromium removal from Modjo Tannery wastewater using Moringa stenopetala seed powder as an adsorbent', Water, Air, & Soil Pollution, 224: 1-10.

Dias, Joana M, Maria CM Alvim-Ferraz, Manuel F Almeida, José Rivera-Utrilla, and Manuel Sánchez-Polo. 2007. 'Waste materials for activated carbon preparation and its use in aqueous-phase treatment: a review', Journal of environmental management, 85: 833-46.

Dinita, Bishnu Joshi Megh Raj Bhatt, Sharma Jarina Joshi Rajani Malla, and Lakshmaiah Sreerama. 2011. 'Lignocellulosic ethanol production: Current practices and recent developments', Biotechnology and Molecular Biology Reviews, 6: 172-82.

Diquarternasi, Yang. 2009. 'Removal of basic blue 3 and reactive orange 16 by adsorption onto quartenized sugar cane bagasse', Malaysian Journal of Analytical Sciences, 13: 185-93.

Division, United Nations Statistic. 2013. 'UNSD Demographic Statistics: Deaths by Age, Sex and Urban/Rural Residence'.

Dutta, Suvanka, Rajnarayan Saha, Harjyoti Kalita, and Achintya N Bezbaruah. 2016. 'Rapid reductive degradation of azo and anthraquinone dyes by nanoscale zero-valent iron', Environmental Technology & Innovation, 5: 176-87.

El-Hendawy, Abdel-Nasser A. 2005. 'Surface and adsorptive properties of carbons prepared from biomass', Applied Surface Science, 252: 287-95.

El-Hendawy, Abdel-Nasser A, SE Samra, and BS Girgis. 2001. 'Adsorption characteristics of activated carbons obtained from corncobs', Colloids and Surfaces A: Physicochemical and Engineering Aspects, 180: 209-21.

Faria, PCC, JJM Orfao, and MFR Pereira. 2004. 'Adsorption of anionic and cationic dyes on activated carbons with different surface chemistries', Water research, 38: 2043-52.

Felista, Mutunga M., Wycliffe C. Wanyonyi, and Gilbert Ongera. 2020. "Adsorption of anionic dye (Reactive Black 5) using macadamia seed husks: kinetics and equilibrium studies." Scientific African 7 : e00283.

Ferraz, Fernanda M, and Qiuyan Yuan. 2020. 'Organic matter removal from landfill leachate by adsorption using spent coffee grounds activated carbon', Sustainable Materials and Technologies, 23: e00141.

Freundlich, H. M. F. 1906. "Uber Die Adsorption in Losungen (Adsorption in Solution)", 57: 384-470.

García, Juan Rafael, Ulises Sedran, Muhammad Abbas Ahmad Zaini, and Zainul Akmar Zakaria. 2018. 'Preparation, characterization, and dye removal study of activated carbon prepared from palm kernel shell', Environmental Science and Pollution Research, 25: 5076-85.

Gatew, Shetie, and Wassie Mersha. 2013. 'Tannery waste water treatment using Moringa stenopetala seed powder extract', Wyno Academic Journal of Physical Science, 1: 1-8.

Girgis, Badie S, Amina A Attia, and Nady A Fathy. 2007. 'Modification in adsorption characteristics of activated carbon produced by H3PO4 under flowing gases', Colloids and Surfaces A: Physicochemical and Engineering Aspects, 299: 79-87.

Girgis, Badie S, Samya S Yunis, and Ashraf M Soliman. 2002. 'Characteristics of activated carbon from peanut hulls in relation to conditions of preparation', Materials Letters, 57: 164-72.

Gong, Renmin, Mei Li, Chao Yang, Yingzhi Sun, and Jian Chen. 2005. "Removal of cationic dyes from aqueous solution by adsorption on peanut hull." Journal of Hazardous Materials 121, no. 1-3 : 247-250.

González-García, P. 2018. 'Activated carbon from lignocellulosics precursors: A review of the synthesis methods, characterization techniques and applications', Renewable and Sustainable Energy Reviews, 82: 1393-414.

Gupta, VK, Alok Mittal, Vibha Gajbe, and Jyoti Mittal. 2008. 'Adsorption of basic fuchsin using waste materials—bottom ash and deoiled soya—as adsorbents', Journal of Colloid and Interface Science, 319: 30-39.

Gürses, Ahmet, Metin Açıkyıldız, Kübra Güneş, and M Sadi Gürses. 2016. 'Classification of dye and pigments.' in, Dyes and pigments (Springer).

Hameed, BH, and FBM Daud. 2008. 'Adsorption studies of basic dye on activated carbon derived from agricultural waste: Hevea brasiliensis seed coat', Chemical Engineering Journal, 139: 48-55.

He, Yang, Jing-Feng Gao, Fang-Qing Feng, Cheng Liu, Yong-Zhen Peng, and Shu-Ying Wang. 2012. 'The comparative study on the rapid decolorization of azo, anthraquinone and triphenylmethane dyes by zero-valent iron', Chemical Engineering Journal, 179: 8-18.

Inyinbor, AA, FA Adekola, and Gabriel Ademola Olatunji. 2016. 'Kinetics, isotherms and thermodynamic modeling of liquid phase adsorption of Rhodamine B dye onto Raphia hookerie fruit epicarp', Water Resources and Industry, 15: 14-27.

Ioannidou, O, and Anastasia Zabaniotou. 2007. 'Agricultural residues as precursors for activated carbon production—a review', Renewable and Sustainable Energy Reviews, 11: 1966-2005.

IUPAC (1972) Manual of Symbols and Terminology for Physicochemical Quantities and Units, London: Butterworths.

Jagtoyen, Marit, and Frank Derbyshire. 1998. 'Activated carbons from yellow poplar and white oak by H3PO4 activation', carbon, 36: 1085-97.

Jahn, Samia Al Azharia. 1991. 'The traditional domestication of a multipurpose tree Moringa stenopetala (Bak. f.) Cuf. in the Ethiopian Rift Valley', Ambio: 244-47.

Janoš, Pavel, Hana Buchtová, and Milena Rýznarová. 2003. 'Sorption of dyes from aqueous solutions onto fly ash', Water research, 37: 4938-44.

Karagöz, Selhan, Turgay Tay, Suat Ucar, and Murat Erdem. 2008. 'Activated carbons from waste biomass by sulfuric acid activation and their use on methylene blue adsorption', Bioresource Technology, 99: 6214-22.

Keane, Jodie, and Dirk Willem te Velde. 2008. 'The role of textile and clothing industries in growth and development strategies', Overseas Development Institute, 7.

Kebede, Temesgen G, Simiso Dube, Vimbai Mhuka, and Mathew M Nindi. 2019. 'Bioremediation of Cd (II), Pb (II) and Cu (II) from industrial effluents by Moringa stenopetala seed husk', Journal of Environmental Science and Health, Part A, 54: 337-51.

Khaled, Azza, Ahmed El Nemr, Amany El-Sikaily, and Ola Abdelwahab. 2009. 'Removal of Direct N Blue-106 from artificial textile dye effluent using activated carbon from orange peel: adsorption isotherm and kinetic studies', Journal of Hazardous Materials, 165: 100-10.

Khatri, Awais, Mazhar Hussain Peerzada, Muhammad Mohsin, and Max White. 2015. 'A review on developments in dyeing cotton fabrics with reactive dyes for reducing effluent pollution', Journal of Cleaner Production, 87: 50-57.

Lagergren, S Kung. 1898. 'About the theory of so-called adsorption of soluble substances', Sven. Vetenskapsakad. Handingarl, 24: 1-39.

Langmuir, Irving. 1916. 'The constitution and fundamental properties of solids and liquids. Part I. Solids', Journal of the American chemical society, 38: 2221-95.

Lee, HV, Sharifah Bee Abd Hamid, and SK Zain. 2014. 'Conversion of lignocellulosic biomass to nanocellulose: structure and chemical process', The Scientific World Journal, 2014.

Liu, Wenjie, Chao Yao, Maohua Wang, Junling Ji, Lin Ying, and Chengyi Fu. 2013. 'Kinetics and thermodynamics characteristics of cationic yellow X-GL adsorption on attapulgite/rice hull-based activated carbon nanocomposites', Environmental Progress & Sustainable Energy, 32: 655-62.

Lori, JA, OM Myina, EJ Ekanem, and AO Lawal. 2010. 'Preliminary evaluation of Moringa oleifera seed shells as precursor for activated carbon', Australian Journal of Basic and Applied Sciences, 4: 5856-61.

Lorimer, JP, TJ Mason, M Plattes, SS Phull, and DJ Walton. 2001. 'Degradation of dye effluent', Pure and Applied Chemistry, 73: 1957-68.

Mahamad, Mohammed Nabil, Muhammad Abbas Ahmad Zaini, and Zainul Akmar Zakaria. 2015. "Preparation and characterization of activated carbon from pineapple waste biomass for dye removal." International Biodeterioration & Biodegradation 102: 274-280.

Mahmoodi, Niyaz Mohammad, Raziyeh Salehi, and Mokhtar Arami. 2011. 'Binary system dye removal from colored textile wastewater using activated carbon: Kinetic and isotherm studies', Desalination, 272: 187-95.

Malik, PK. 2004. 'Dye removal from wastewater using activated carbon developed from sawdust: adsorption equilibrium and kinetics', Journal of Hazardous Materials, 113: 81-88.

Marsh, Harry, and Francisco Rodríguez Reinoso. 2006. Activated carbon (Elsevier).

Melaku, Yadessa, Norbert Arnold, Juergen Schmidt, and Ermias Dagne. 2017. 'Analysis of the husk and kernel of the seeds of Moringa stenopetala', Bulletin of the Chemical Society of Ethiopia, 31: 107-13.

Mimi, C. Yu, Paul L. Skipper, Steven R. Tannenbaum, Kenneth K. Chan, and Ronald K. Ross. 2002. "Arylamine exposures and bladder cancer risk." Mutation Research/Fundamental and Molecular Mechanisms of Mutagenesis, 506: 21-28.

Moreno-Castilla, Carlos. 2004. 'Adsorption of organic molecules from aqueous solutions on carbon materials', Carbon, 42: 83-94.

Mottaleb, Mohammad A, and David Littlejohn. 2001. 'Application of an HPLC-FTIR modified thermospray interface for analysis of dye samples', Analytical Sciences, 17: 429-34.

Muhammad, N, P Jeremy, P Michael, D Smith, and AD Wheatley. 1998. "Sanitation and water for all." In 24th WEDC Conference, Islamabad, Pakistan, 346-49.

Mui, Edward LK, WH Cheung, Marjorie Valix, and Gordon McKay. 2010. 'Dye adsorption onto char from bamboo', Journal of Hazardous Materials, 177: 1001-05.

Nakagawa, Yoshiteru, Miguel Molina-Sabio, and Francisco Rodríguez-Reinoso. 2007. 'Modification of the porous structure along the preparation of activated carbon monoliths with H3PO4 and ZnCl2', Microporous and Mesoporous Materials, 103: 29-34.

Namasivayam, C., R. Radhika, and S. Suba. 2001. "Uptake of dyes by a promising locally available agricultural solid waste: coir pith." Waste management 21, no. 4: 381-387.

Namasivayam, C, and Dyes Kavitha. 2002. 'Removal of Congo Red from water by adsorption onto activated carbon prepared from coir pith, an agricultural solid waste', Dyes and pigments, 54: 47-58.

Oluyori, Abimbola P, Arun Kumar Shaw, Rastogi Preeti, Sammajay Reddy, Olubunmi Atolani, Gabriel A Olatunji, and Oluwatoyin A Fabiyi. 2016. 'Natural antifungal compounds from the peels of Ipomoea batatas Lam', Natural product research, 30: 2125-29.

Pagga, Udo, and Derek Brown. 1986. 'The degradation of dyestuffs: Part II Behaviour of dyestuffs in aerobic biodegradation tests', Chemosphere, 15: 479-91.

Peláez-Cid, Alejandra-Alicia, Ana-María Herrera-González, Martín Salazar-Villanueva, and Alejandro Bautista-Hernández. 2016. 'Elimination of textile dyes using activated carbons prepared from vegetable residues and their characterization', Journal of environmental management, 181: 269-78.

Pierce, Jeff. 1994. 'Colour in textile effluents-the origins of the problem', Journal of the Society of Dyers and Colourists, 110: 131-33.

Ramakrishna, Konduru R, and T Viraraghavan. 1997. 'Dye removal using low cost adsorbents', Water science and technology, 36: 189-96.

Rashed, Mohamed Nageeb. 2013. 'Adsorption technique for the removal of organic pollutants from water and wastewater', Organic pollutants-monitoring, risk and treatment, 7: 167-94.

Reffas, A, V Bernardet, B David, L Reinert, M Bencheikh Lehocine, M Dubois, N Batisse, and L Duclaux. 2010. 'Carbons prepared from coffee grounds by H3PO4 activation: Characterization and adsorption of methylene blue and Nylosan Red N-2RBL', Journal of Hazardous Materials, 175: 779-88.

Reisch, Marc S. 1996. 'Asian textile dye makers are a growing power in changing market', Chemical & Engineering News, 74: 10-12.

Rivera-Utrilla, J, Isidora Bautista-Toledo, M A Ferro-García, and C Moreno-Castilla. 2001. 'Activated carbon surface modifications by adsorption of bacteria and their effect on aqueous lead adsorption', Journal of Chemical Technology & Biotechnology, 76: 1209-15.

Robert, L, F Joseph, and A Alexander. 2008. 'Fisher's contact dermatitis in textiles and shoes', BC Decker Inc, Ontario: 339-401.

Robinson, Tim, Geoff McMullan, Roger Marchant, and Poonam Nigam. 2001. 'Remediation of dyes in textile effluent: a critical review on current treatment technologies with a proposed alternative', Bioresource Technology, 77: 247-55.

Rodriguez-Reinoso, Francisco. 1998. 'The role of carbon materials in heterogeneous catalysis', Carbon, 36: 159-75.

Rouquerol, J., D. Avnir, C. W. Fairbridge, D. H. Everett, J. M. Haynes, N. Pernicone, J. D. F. Ramsay, K. S. W. Sing, and K. K. Unger. 1994. "Recommendations for the characterization of porous solids (Technical Report)." Pure and applied chemistry 66, no. 8: 1739-1758.

Santhy, K, and P Selvapathy. 2006. 'Removal of reactive dyes from wastewater by adsorption on coir pith activated carbon', Bioresource Technology, 97: 1329-36.

Sepulveda, Luisa Antonia, and Cesar Costapinto Santana. 2013. 'Effect of solution temperature, pH and ionic strength on dye adsorption onto Magellanic peat', Environmental technology, 34: 967-77.

Sharma, YC, and SN Upadhyay. 2011. 'An economically viable removal of methylene blue by adsorption on activated carbon prepared from rice husk', The Canadian Journal of Chemical Engineering, 89: 377-83.

Smith, K. M., G. D. Fowler, S. Pullket, and N_J D. Graham. 2009. "Sewage sludge-based adsorbents: a review of their production, properties and use in water treatment applications." Water research 43, no. 10 : 2569-2594.

Tareq, Rizwan, Nahida Akter, and Md Shafiul Azam. 2019. 'Biochars and biochar composites: low-cost adsorbents for environmental remediation.' in, Biochar from biomass and waste (Elsevier).

Tehrani, Nima Fotouhi, Javier S Aznar, and Yohannes Kiros. 2015. 'Coffee extract residue for production of ethanol and activated carbons', Journal of Cleaner Production, 91: 64-70.

US EPA. 1996. "Best management practices for pollution prevention in the textile industry."

Valko, Emery I. 1957. 'The theory of dyeing cellulosic fibers', Textile Research Journal, 27: 883-98.

Vandevivere, Philippe C, Roberto Bianchi, and Willy Verstraete. 1998. 'Treatment and reuse of wastewater from the textile wet-processing industry: Review of emerging technologies', Journal of Chemical Technology & Biotechnology: International Research in Process, Environmental and Clean Technology, 72: 289-302.

Wang, Zongping, Miaomiao Xue, Kai Huang, and Zizheng Liu. 2011. 'Textile dyeing wastewater treatment', Advances in treating textile effluent, 5: 91-116.

Weber, Thomas W, and Ranjit K Chakravorti. 1974. 'Pore and solid diffusion models for fixed-bed adsorbers', AIChE Journal, 20: 228-38.

Worch, E. 'Adsorption Technology in Water Treatment Fundamentals, Processes, and Modeling, 2012 Walter de Gruyter GmbH & Co', KG, Berlin/Boston: 3.

Yahya, Mohd Adib, Zakaria Al-Qodah, and CW Zanariah Ngah. 2015. 'Agricultural bio-waste materials as potential sustainable precursors used for activated carbon production: A review', Renewable and Sustainable Energy Reviews, 46: 218-35.

Yaseen, DA, and M Scholz. 2019. 'Textile dye wastewater characteristics and constituents of synthetic effluents: a critical review', International journal of environmental science and technology, 16: 1193-226.

Zuo, Songlin, Jianxiao Yang, and Junli Liu. 2010. 'Effects of the heating history of impregnated lignocellulosic material on pore development during phosphoric acid activation', Carbon, 48: 3293-95.